TU Delft Delft University of Technology

Fouling control in ceramic nanofiltration membrane by pre-coating with calcium carbonate

Yidan Xu

Fouling control in ceramic nanofiltration membrane by pre-coating with calcium carbonate

by

Yidan Xu

In partial fulfillment of requirements for the degree of

Master of Science

in Civil Engineering

at the Delft University of Technology,

to be defended online on Thursday, September 29, 2022, at 9:30 AM.

Assessment committee:	Prof. dr. ir. L. C. Rietveld,	TU Delft
	Dr. ir. S. G. J. Heijman,	TU Delft
	Dr. ir. C. Chassagne,	TU Delft
	Ir. Y.Li	TU Delft

Abstract

Water scarcity and uneven distribution of water resources pose a significant challenge globally. Searching for alternative water resources could alleviate this issue. Municipal sewage reclamation with ceramic NF membrane has gained momentum nowadays. However, the inevitable fouling, especially organic fouling during membrane filtration, is the major limitation of the application. To mitigate the fouling issues and protect the membrane from frequent sodium hypochlorite cleaning, a reaction-based $CaCO_3$ pre-coating method, which could prevent the direct contact of foulant and ceramic NF surface was developed. Acid cleaning was applied to initiate the reaction between $CaCO_3$, which was attached with foulants (sodium alginate) and acid. Lastly, forward flush was implemented to remove the loosened $CaCO_3$ and sodium alginate layers.

The effectiveness of hydrochloric acid cleaning, formic acid cleaning and citric acid cleaning was studied in this paper. Citric acid was found to be the most effective way of cleaning because of the highest permeability recovery rate obtained and the lowest consumption rate of the pre-coating layer. This could be ascribed to the carboxyl groups chelation with calcium ions and the 'peeled' chelates adsorbed with more foulants were flushed away. Formic acid was less efficient showing moderate efficiency. Besides, HCl cleaning restored the lowest extent of membrane permeability. Additionally, experiments of increasing the pre-coated $CaCO_3$ amount (7655 mg/m^2) to apply for more filtration/acid cleaning cycles were executed. The effectiveness increases in the order of HCl, formic acid and citric acid. The pre-coated membrane cleaned with citric acid could last for the whole six cycles, while the membrane cleaned with HCl only worked in the first three cycles. Lastly, the effect of bubbles generated during the reaction was explored using $CaHPO_4$ as a pre-coating layer. However, the hypothesized positive impact of bubbles was not verified.

Acknowledgment

With the complement of this thesis, my story with TU Delft is about to end in the summer of 2022. I have received lots of support from many people during my two-year life at TU Delft.

Firstly, my deepest and sincerest gratitude goes to my supervisor Dr. ir. S. G. J. Heijman for his continuous guidance throughout my research. And I would like to thank Prof. dr. ir. L. C. Rietveld, who gave me invaluable feedback to improve my reports. Dr. ir. C. Chassagne's constructive suggestion urged me to think deeper about my report, thank you a lot! I would like to express my thanks to my daily supervisor ir. Y. Li. I would never finish this report without his patient help throughout my graduation project.

I also want to thank my cheerful friends: Luqianxue Zhang, Yiqian Wu, Yuhao Wu, Haozheng Lyu, and Hao Li. Luqianxue and Hao were always willing to share their findings and discuss them with me, inspiring me a lot! My boyfriend Sihan, you shed a light on me and encouraged me whenever I was under pressure and anxiety. Thank you! Finally, I would like to express my love and gratitude to my family. Your support and love were my motivation to move forward!

Yidan Xu,

September, 2022

Content

List of Figures

List of Tables

List of Abbreviations

UF	Ultrafiltration
MF	Microfiltration
NF	Nanofiltration
RO	Reverse osmosis
FO	Forward osmosis
ED	Electrodialysis
TMP	Transmembrane pressure
OM	Organic matter
AOM	Algal organic matter
EfOM	Effluent organic matter
SMP	Soluble microbial products
NOM	Natural organic matter
HS	Humic substances
BAP	Biomass-associated products
UAP	Utilization-associated products
MW	Molecular weight
PAC	Powdered activated carbon
PDI	Potential determining ions
SA	Sodium alginate

1. Introduction

1.1 Research background

With the explosion of population and the progress of industrialization, the demand for clean water is increasing. However, the uneven distribution of water resources and water scarcity worldwide have driven the search for alternative water resources (Chen et al., 2003; Goh et al., 2018). There are two general ways to alleviate these issues: seawater desalination and wastewater reclamation. Despite the development of seawater desalination technology, the high cost is still a limiting factor. Therefore, wastewater reclamation has attracted more attention and is becoming one of the key research topics today (Chen et al., 2003). Municipal sewage reclamation has become a reliable water supply due to the relatively constant production, attributed to its dependency on municipal sewage production and low propensity to be affected by precipitation (Wintgens et al., 2005). Membrane technology is in the limelight and has been applied in various fields, including water reclamation. It is superior to conventional treatments due to its lower footprint and high separation efficiency. Ceramic nanofiltration (NF) membranes are regarded as a suitable process for municipal sewage reclamation as they exhibit better chemical and thermal resistance and mechanical strength properties than polymeric NF membranes.

The problem is that the fouling phenomenon is inevitable in membrane separation, especially for ceramic NF membranes, as they are susceptible to backwash. Therefore, NF membranes need to be cleaned occasionally to relieve and resolve fouling problems. Membranes can be cleaned both physically and chemically. Physical cleaning mainly refers to forward flush and backwash (more effective than forwards flush) but a previous study showed that backwash would damage the edge of ceramic membranes (Figure 1.1); thus, hydraulic cleaning is not suitable (Kramer et al., 2020). As for chemical cleaning, a long-term dose of chemicals like sodium hypochlorite would deteriorate the glass seal layer of ceramic membranes (Kramer et al., 2020). Therefore, more efficient and moderate cleaning methods should be investigated. A practical

approach to remove the organic foulants is to pre-coat the membrane with particle suspension. Foulants can be attached to the pre-coating layer, while water can penetrate the pre-coating layer as it is permeable and incompressible. It is easily removable that foulants with the pre-coating layer can be cleaned by forward flush and backwash (Galjaard, Buijs, et al., 2001). This technology prevents direct contact between foulants and the membrane surface, and decreases the frequency of sodium hypochlorite dosing. However, pre-coating to control fouling problems is more applied in MF/UF and the study on its application on ceramic NF is limited. Additionally, a preliminary experiment by Kramer et al. (2020) proved that backwash is not applicable. Hence in this paper, the cleaning of the pre-coating layer and foulant is focused on acid cleaning and chemical dosing.

Figure 1.1 Damage to the edge of ceramic NF membrane after backwashing (adapted from Kramer et al., 2020)

1.2 Previous research and knowledge gap

The preliminary research on reaction-based pre-coat technology of ceramic NF membrane has been done by Kramer et al. (2020). Pre-coat method using calcium carbonate particles and Fenton reaction to remove sodium alginate as foulants were tested. Results showed that pre-coating with calcium carbonate exhibited higher foulant removal and net water production. Two acids: hydrochloric acid (Eq.1) and citric acid (Eq.2 and 3), were applied to remove foulants and the pre-coating layer in the calcium

carbonate experiment.

$$CaCO_3(s) + 2H^+ \rightarrow Ca^{2+} + H_2O + CO_2(g) \quad (1.1)$$

$$3CaCO_3(s) + 2(CH_2COOH)_2C(OH)COOH \rightarrow Ca_3((CH_2COO)_2C(OH)COO)_2 + 6H^+ + 3CO_3^{2-} \quad (1.2)$$

$$H_2CO_3(aq) \rightarrow H_2O + CO_2(g) \quad (1.3)$$

When cleaned with citric acid, the permeability can be recovered to 76%, whereas an increase of 12% for permeability dosing hydrochloric acid was obtained. It was assumed that acid strength could affect the reaction. Hydrogen ions were converted and pH increased during the reaction between calcium carbonate and strong acid HCl, thus hindering the reaction consequently (Kramer et al., 2020). The preliminary results displayed that citric acid might be more effective with calcium carbonate pre-coating layer cleaning, but the effects of different acid dosing still need to be probed. Additionally, the optimized conditions for the pre-coat/acid cleaning cycle remained undetermined.

1.3 Research questions

The main objective of this study is to explore the potential of fouling control of ceramic NF membranes with calcium carbonate pre-coating method. The following questions help get a deeper understanding of this study.

1. What is the effect of different acid cleaning (formic acid, citric acid, and hydrochloric acid)?

2. How many effective cycles can last for the pre-coating fouling test?

3. What is the influence of carbon dioxide bubbles during the acid cleaning process?

To answer the above questions, this research is divided into the following 5 sections:

Chapter 2: literature review:

This section elucidates the application of ceramic nanofiltration membrane on municipal sewage reclamation, the fouling phenomenon with the application and fouling control and cleaning methods. A literature evaluation is contained at the end to explain the importance of this study.

Chapter 3: methodology

This section entails the detailed experiment design to answer the research questions. The experiments were mainly divided into three parts. Firstly, the comparisons between acids cleaning on pristine membranes and $CaCO_3$ pre-coated membranes were conducted. Then to explore the efficiency of cleaning with three acids, filtration/cleaning experiments were implemented on the $CaCO_3$ pre-coated membranes using sodium alginate as foulants for three runs and six runs, respectively. Lastly, the same amount of $CaHPO_4$ was dosed on the pristine membrane as a control group to detect the impact of bubbles generated when $CaCO_3$ was applied as the pre-coating layer.

Chapter 4: Results and discussions

Four results, including the effectiveness of acid cleaning on reaction-cased pre-coated membranes, efficiencies of different acids in three filtration/cleaning cycles and six cycles on $CaCO_3$ pre-coated membranes and the impact of generated bubbles during acid cleaning on CaCO3 pre-coated membraned are illustrated here. Potential causes of the obtained consequences are elucidated in this chapter.

Chapter 5: Conclusions

Conclusions are drawn according to the last chapter and the main findings with brief

explanations will be summarized to answer the research questions.

Chapter 6: Recommendations

In this last section, several recommendations for future experiments are advocated to improve the effectiveness of this study in real applications.

2. Literature review

2.1 Municipal sewage reclamation

As a result of the cumulative effects of population explosion and climate change, the natural water compensation rate is much lower than the water resources shrink rate. (Gude, 2017). Moreover, severe droughts, expansion of land use, disparities in water distributions worldwide, and ecological and geological system changes caused by anthropogenic activities like urbanization and overexploitation, have made fresh water supply unable to meet the escalating water demand (Gude, 2017; Hube et al., 2020; Wu et al., 2021).

Brackish water and seawater desalination, and water reclamation would help address global water scarcity issues. Despite that seawater desalination technology is rapidly developed, the high cost and its consumption of existing natural water resources have limited its sustainable application (Chen et al., 2003; Wu et al., 2021). Therefore, attention has been paid to water reuse and reclamation. Both industrial wastewater and municipal sewage could be reclaimed mostly for non-potable use. Wintgens et al. (2005) stated that reclaimed municipal sewage was a reliable water resource for its relatively constant production being independent of precipitation, and through reusing wastewater, the natural recirculation of water resources could be shortened.

Substantive treatment processes have been proposed to meet the strict water quality of reclaimed sewage. There are mainly two types of treating methods: natural system and engineered approach (Gude, 2017). Natural treatments, including wetlands and soil aquifer treatment, are less preferred considering its limitation on climate and hydrogeology (Gude, 2017). Engineered approaches are designed in accordance with the chemical and physical properties of the contaminants in wastewater, which contains sand filtration, membrane technology, coagulation, etc. (Gude, 2017). Membrane separation technology has been the major means since the 1990s as it consumes less energy with higher efficiency and less footprint (Gude, 2017; Wu et al., 2021).

2.2 Membrane separation technology

Membranes act as a barrier to separate contaminants and clean water by size exclusion, adsorption, and electrostatic repulsion (Asif & Zhang, 2021). The different transport rates of the impurities, which depend on different driving forces, through the membrane surfaces lead to the separation processes (Strathmann, 1981). Pressure-driven membranes could be classified into four types according to the pore size: microfiltration (MF) membranes, ultrafiltration (UF) membranes, nanofiltration (NF) membranes, and reverse osmosis (RO) membranes. Table 2.1 displays the specification of pressure-driven membranes. Furthermore, the pressure-driven membranes are categorized into polymeric membranes and ceramic membranes in accordance with effective filtration materials applied. Polymeric membranes are prone to chemical cleaning under some extreme conditions. Decreasing the concentration of cleaning agents would alleviate this issue but the cleaning time is increased consequently (Kramer et al., 2015). As a result, polymeric pressure-driven membranes are not economical if applied in wastewater reclamation. Osmotic-driven membranes refer to forward osmosis (FO) membranes, which can operate without extra pressure hence saving energy. However, water reclamation with FO membranes is limited due to its relatively low flux (Kramer et al., 2015). Additionally, the requirements for relatively high ion concentration in the draw solution, so RO membranes are needed, which consumes much energy (Kramer et al., 2015). Electrodialysis (ED) membranes are electrical-driven separation membranes with an electric potential difference. Several lines of evidence suggest that increasing the electric voltage and current density improves ED effectiveness. However, the longevity of the membranes would be decreased as a result of higher electrical resistance (Hube et al., 2020).

Collectively, the application of ceramic pressure-driven membranes, which is more robust, is in the limelight in municipal sewage reclamation applications.

Table 2.1 Classification of pressure-driven membranes (adapted from Gude, 2017)

Membrane type	Particle capture size	Typical contaminants removed	Typical operation pressure ranges
MF	0.1-10 μm	Suspended solids, bacteria, protozoa	0.1-2 bar
UF	ca. 0.003-0.1 μm	Colloids, proteins, polysaccharides, most bacteria, viruses (partially)	1-5 bar (cross-flow) 0.2-0.3 bar (dead-end and submerged)
NF	ca. 0.001 μm	Viruses, natural organic matter, multivalent ions	5-20 bar
RO	ca. 0.001 μm	Almost all impurities, including monovalent ions	10-100bar

2.3 Ceramic membranes

Ceramic membranes are typically asymmetric structured, made of multilayers of one or several ceramic materials (Figure 2.1a) when applied in wastewater and water treatment processes: support (substrate) layer, intermediate layer(s), and separation (selective) layer (Asif & Zhang, 2021; C. Li et al., 2020). The microporous substrate layer is made from metal oxides, such as alumina (Al_2O_3), titanium oxide (TiO_2), zirconia (ZrO_2), silica dioxide (SiO_2), and silica carbide (SiC) (Asif & Zhang, 2021; Kim & van der Bruggen, 2010; C. Li et al., 2020). The properties of different selective layers of ceramic membranes are displayed in Figure 2.1b. Among the above membranes, ceramic membranes fabricated by Al_2O_3 are mostly commercially applied for their lowest cost but with relatively poor chemical stability compared to TiO_2 ceramic membranes (Asif & Zhang, 2021; C. Li et al., 2020).

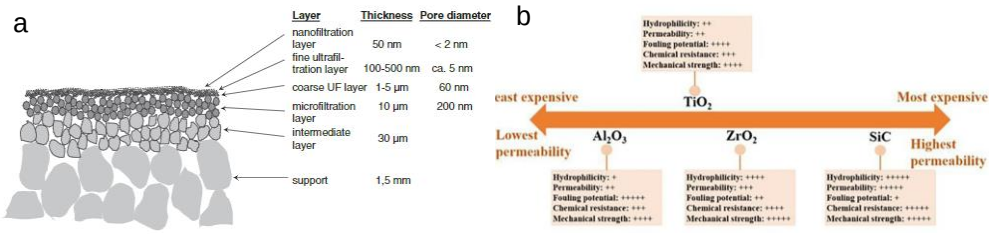

Figure 2.1 (a) The schematic diagram of ceramic membranes (adapted from Benfer et al., 2004); (b) and the features of ceramic membranes with different selective layers (adapted from Asif & Zhang, 2021).

Ceramic membranes are generally divided into three types by their geometry: tubular, hollow fiber and flat sheet ceramic membranes. Tubular and hollow fiber membranes are more widely applied in wastewater treatment due to their high specific surface area and packing density (Arumugham et al., 2021), and high mechanical stability (Asif & Zhang, 2021).

Ceramic membranes possess advantages over polymeric membranes owing to their high thermal, mechanical and thermal resistances, and lower fouling performances (Asif & Zhang, 2021; Li et al., 2020). Besides, NF membranes are more hydrophilic than UF (Wu et al., 2021), that hydrophilicity is related to lower fouling (Hofs et al., 2011). NF membranes have a smaller molecular weight cut-off (MWCO) from 200-1000 Da, hence are more applicable to removing coloring agents, mineral ions, and trace organic molecules from wastewater (Combe et al., 1997). Therefore, ceramic NF membranes which are less susceptible to organic fouling, have gained much momentum in municipal sewage reclamation (Kramer et al., 2020; C. Li et al., 2020).

2.4 Fouling phenomenon in ceramic NF membranes

The fouling phenomenon, which would decrease clean water production, is an inevitable issue during membrane separation processes, although ceramic membranes

are less prone to fouling. There are two types of fouling, i.e., reversible fouling and irreversible fouling. Reversible fouling could be physically removed and backwashable, while irreversible fouling can only be cleaned by chemicals (Guo et al., 2012; Zhao et al., 2018).

2.4.1 Fouling mechanisms

Previous studies have established four main fouling mechanisms: complete pore blocking, intermediate blocking, standard blocking, and cake filtration (Griffiths et al., 2014; Kirschner et al., 2019).

Complete pore blocking refers to the deposition of larger foulant particles on the membranes and covering the pores, that these foulants do not precipitate on each other (Griffiths et al., 2014; Kirschner et al., 2019). Intermediate blocking is defined as the foulant particles landing on membrane surfaces and are allowed to deposit on the previous particles, thus partially covering the channels (Griffiths et al., 2014; Kirschner et al., 2019). Unlike the previous two mechanisms, standard blocking happens inside the pores rather than on membrane surfaces where smaller foulants adhere to the pores, decreasing pore diameter (Griffiths et al., 2014; Kirschner et al., 2019). In the case of cake filtration, a permeable and porous cake layer is formed with the accumulation of foulants on membrane surfaces, giving rise to increased total membrane resistance (Griffiths et al., 2014; Kirschner et al., 2019).

2.4.2 Major foulants of ceramic nanofiltration membranes

Foulants can be classified into four groups which are inorganic foulants, particulate substances, organic foulants and biological organisms (Guo et al., 2012; Listiarini et al., 2009). Inorganic fouling mainly refers to the precipitation of minerals ions, for instance, calcium, iron, carbonate, etc., caused by the hydrolysis or oxidation processes (Goh et al., 2018; Guo et al., 2012). The physical blockage caused by particles or colloids in feed water is considered particulate fouling. Smaller particles could result in pore

blocking, while larger particles deposit on the membrane surfaces and accumulate to form a cake layer (Guo et al., 2012; Wintgens et al., 2005). Organic fouling and biofouling are regarded as the dominant causes of nanofiltration membranes (Q. Li & Elimelech, 2004; Listiarini et al., 2009; Mohammad et al., 2015). However, ceramic NF membranes exhibit a lower propensity to be affected by chlorine (which is effective for biofouling alleviation) that it can remain membrane integrity after chlorine dosing (C. Li et al., 2020). Therefore, biofouling is less recalcitrant than organic fouling in ceramic NF membranes. To get a better understanding of fouling in ceramic NF membranes, the following subsection gives a detailed overview of organic fouling.

Organic fouling is related to the bulk organic matter (OM) in the feed water, which could be simply classified as microbially-derived OM and terrestrially-derived OM (Amy, 2008). Microbially-derived OM contains autochthonous or algal organic matter (AOM), which consists of extra/intracellular macromolecules and cell debris, and wastewater effluent organic matter (EfOM) which includes refractory OM, trace synthetic organic compounds and soluble microbial products (SMP) (Amy, 2008; Jarusutthirak & Amy, 2006; Ke et al., 2013). The major components of terrestrially-derived natural organic matter (NOM) are humic substances (HS) (Amy, 2008; Guo et al., 2012). It has been conclusively shown that there are at least three fouling mechanisms of organic fouling. NOM could adsorb on membrane pores, decreasing the pore diameter; or NOM could deposit on the membrane surfaces forming a gel layer (Guo et al., 2012). When particles are present with NOM, they would be bound by NOM forming a particle/NOM layer (Guo et al., 2012).

In wastewater reclamation, SMP, the majority of EfOM, is regarded as the cause of severe fouling (Jarusutthirak & Amy, 2006; Ke et al., 2013). SMP are secreted by microorganisms and derived into two groups: biomass-associated products (BAP) and utilization-associated products (UAP) (Jarusutthirak & Amy, 2007). The components of SMP were found to mainly contain polysaccharides, proteins, fatty acids and organic

colloids (Jarusutthirak & Amy, 2007; Ke et al., 2013). Among them, polysaccharides have been found as the predominant substances related to serious fouling phenomena (Amy, 2008).

Sodium alginate (structure depicted in Figure 2.2a) is usually used as the surrogate of polysaccharides. It is known to form a three-dimensional gel network with the presence of divalent ions like Ca^{2+}. Ca^{2+} preferentially binds with the carboxyl groups of sodium alginate, thus bridging the adjacent molecules, forming the so-called "egg-box" model (elucidated in Figure 2.2b).

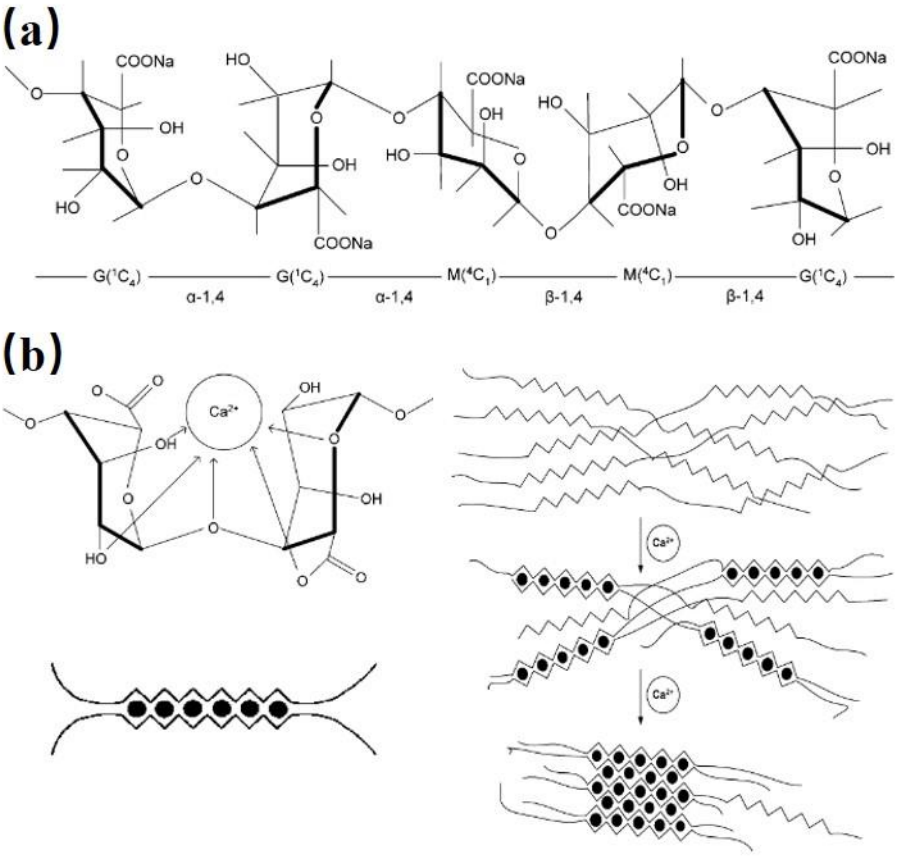

Figure 2.2 schematic structure of (a) sodium alginate, and (b) the formation of an egg-box model of sodium alginate with Ca^{2+} (adapted from Katsoufidou et al., 2007)

2.5 Fouling prevention and mitigation

It is concluded that the occurrence of fouling is detrimental to the membrane separation process. Membrane fouling increases operational energy consumption, reduces clean

water production, shortens membrane longevity and decreases the foulant retention rate (Ke et al., 2013; Zhao et al., 2018). Therefore, efforts have been put into the prevention and mitigation of fouling issues. Generally, fouling control could be classified into prevention (design improvements to avoid fouling phenomenon) and mitigation (cleaning after fouling occurs) methods.

2.5.1 Fouling prevention

a). Membrane modification

Fouling could be affected by the membrane properties like hydrophilicity, surface roughness, surface charge and pore size, etc. (Mohammad et al., 2015; Sun et al., 2013; Wu et al., 2021). Previous research on surface modification showed that grafting is an effective way to replace the surface functional groups (e.g. hydroxyl group) with other groups like methyl groups (by the Grignard process) and organosilanes (by silanization process (Asif & Zhang, 2021; C. Li et al., 2020; Mustafa et al., 2014). Nevertheless, the above grafting methods resulted in a decrease in permeate even though the antifouling properties of the grafted ceramic membranes have been improved (Asif & Zhang, 2021; C. Li et al., 2020; Mustafa et al., 2014).

b). Pretreatment

There are several pretreatment processes to decrease the accumulation of foulants on membranes or to change the interactions between foulants and membrane surfaces (Sun et al., 2013). Coagulation-sedimentation process is reported as an effective way for hydrophobic organic matter with high MW and particles (Sun et al., 2013; Wu et al., 2021). Coagulants are added to neutralize the charge of foulants and change the size of pollutants (W. Gao et al., 2011). However, the residual ions after the coagulation process remains a problem with NF, decreasing removal efficiency (Wang, Tang, et al., 2020). Ozonation is also applied as powerful oxidation of macromolecular organic matter into smaller molecules or inorganic matters (Sun et al., 2013). This way, the concentration of foulants could be reduced and ozonation also helps alleviate the

adhesion of foulants on the surface (You et al., 2007). Activated carbon adsorption is usually combined with low-pressure membranes to decrease the pore blocking and cake layer resistance (Wang, Tang, et al., 2020). The sufficient adsorption area of powdered activated carbon (PAC) has made it a promising adsorbent with high removal efficiency (W. Gao et al., 2011).

2.5.2 Hydraulic flush

a). Forward flush

Clean water is applied to rinse the membrane surface and flush away the attached foulant layers. Water enters the system by the feed side with a high cross-flow velocity (Lee et al., 2015; Zhang et al., 2015). Kramar et al. (2020) suggested that a relatively low cross-flow velocity is sufficient for ceramic NF membrane because of the weak interactions between foulants and membrane surface.

b). Backwash

Backwash is reported to be more efficient for sodium alginate removal compared with humic acid (W. Gao et al., 2011). Unlike forward flush, backwash of clean water enters the system by the permeate side with high pressure, which helps dislodge the pollutants in the pores. However, the backwash of ceramic NF membrane may not be applicable because former research has proved the damage to its glass seal layer after backwash (Kramer et al., 2020).

2.5.3 Chemical cleaning

Chemical cleaning is applied to remove irreversible fouling after the permeate flux has decreased by 50-60% (Lee et al., 2015). There are mainly three types of chemicals: acids, bases, and oxidants.

a). Acids cleaning

Mineral acids, for instance, hydrochloric acid (HCl) and sulphuric acid (H_2SO_4) are widely applied for inorganic fouling mitigation and multivalent cationic particle removal (Porcelli & Judd, 2010). As well as mineral acids, organic acids like citric acids and oxalic acids are more effective for the removal of organo-metallic foulants by chelation reaction (Porcelli & Judd, 2010).

b). Base cleaning

Sodium hydroxide (NaOH) solution is applied in the case of organic fouling to dissolve weakly acidic organic matter or break down high MW polysaccharides and proteins into smaller molecules (Porcelli & Judd, 2010). Additionally, it is effective for inorganic colloids and silicates cleaning (Porcelli & Judd, 2010).

c). Oxidants cleaning

The commonly used oxidants are hydrogen peroxide (H_2O_2) and sodium hypochlorite (NaOCl), which are applied for the improved removal of organic fouling (Lee et al., 2015). The functional groups of NOM are degraded by oxidants to carboxyl, ketonic and aldehydes groups, which are more easily removed under alkaline conditions, hence caustic soda is usually coupled with oxidants cleaning (Porcelli & Judd, 2010).

However, the abovementioned antifouling technologies have their drawback during applications. For example, NaOCl cleaning is detrimental to membranes that some polymeric membranes are not chlorine-resistant, and even ceramic membranes would be damaged after long-term use of it. Pretreatment of membranes cannot completely clean the organic fouling of the membrane (Wang et al., 2020). Therefore, novel fouling mitigation methods are of great interest in the research.

2.5.4 Dynamic membrane

Dynamic membrane (DM) refers to the cake layer formed by pre-deposited particles on the pristine membrane before filtration, acting as a beneficial antifouling membrane

(Anantharaman et al., 2020; Wang et al., 2020). According to the size of deposited particles, DMs is classified into three class: Class I (membrane pore size lesser than particles), Class II (membrane pore size much larger than particles), and Class III (membrane pore size similar to particles), among which Class I DMs has gained more attention in the field of organic foulants removal recently (Anantharaman et al., 2020). Anantharamam et al. (2020) reviewed several merits of DM compared with conventional antifouling technologies. Notably, DMs perform higher NOM rejection rates and better fouling mitigation than the pre-adsorption/coagulation step of membrane filtration as DM circumvents direct contact between pristine membrane surface and foulants (Anantharaman et al., 2020; Galjaard, van Paassen, et al., 2001). Moreover, its greater uniformity guaranteed higher rejection rates than modified membranes (Anantharaman et al., 2020).

Galjaard et al. (2001) applied Enhanced Pre-Coat Engineering (EPCE) on polymeric MF/UF, where several types of particles were selected as a pre-coating layer. The mechanism of EPCE is depicted in Figure 2.3. Firstly, the pristine membrane was pre-coated with particle suspension to prevent the direct deposition of gel-like foulants on the membrane surface. The pre-coating layer was permeable and could be easily removed. Then, the fouling filtration step starts after the pre-coating step when foulants would deposit and attach to the pre-coated layer. Finally, backwash was implemented to relieve the increased transmembrane pressure (TMP) by detaching the polluted layer. Galjaard et al. (2001) reported that permeability was restored well with pre-coated membranes and is a promising method to improve the antifouling of membranes for more operation cycles.

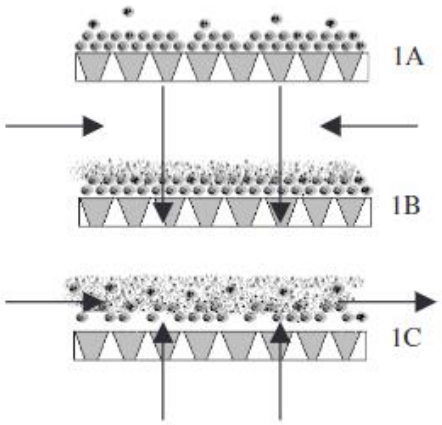

Figure 2.3 Schematic diagram of EPCE (adapted from Galjaard et al., 2003): (1A) Deposition of particle suspension on the membrane surface; (1B) fouling filtration of the pre-coated membrane; (1C) and backwashing for the lifting and removal of foulant attached pre-coating layer.

As a commercially available, biodegradable and cheap substance, $CaCO_3$ was selected as a possible dynamic membrane component (B. Gao et al., 2013). Al-Malack & Anderson (1998) tested the feasibility of $CaCO_3$ pre-coated polymeric MF membrane to treat secondary effluent. It was reported that 1350 mg/L $CaCO_3$ circulated for 30 minutes could form the dynamic membrane on the MF membrane to narrow the selective pore size, hence perform a stable flux production and low turbidity of the effluent (Al-Malack & Anderson, 1998). $CaCO_3$ pre-coated membrane could also be applied in the removal of halogenated substances in the water (B. Gao et al., 2013). The pre-deposited nano-sized $CaCO_3$ on the membrane with photocatalyst promoted COD removal rate and dehalogenation efficiencies (B. Gao et al., 2013).

Beside the application of $CaCO_3$ on polymer MF/UF membrane, Kramer et al. (2020) have applied EPCE on $CaCO_3$ pre-coated ceramic NF membranes for municipal wastewater reclamation on the lab scale. To make EPCE more viable on ceramic NF membranes, the reaction-based cleaning followed by forward flush was applied instead of backwash after membrane fouling (a schematic diagram of calcium carbonate pre-coated membrane is shown in Figure 2.4). Fenton reaction-based pre-coating and

calcium carbonate ($CaCO_3$) with acid reaction-based pre-coating were tested. It is concluded that $CaCO_3$ nanoparticle pre-coated membranes with citric cleaning exhibited relatively high permeability recovery (about 76%) and the highest net water production under constant pressure filtration mode. Like Galjaard et al.'s study (2001), the pre-coat layer was regenerated after each filtration/cleaning cycle. However, the cleaning efficiency was unexpectedly lower than the former cycle due to remaining foulants would decrease the stability of redeposited $CaCO_3$ Kramer et al. (2020).

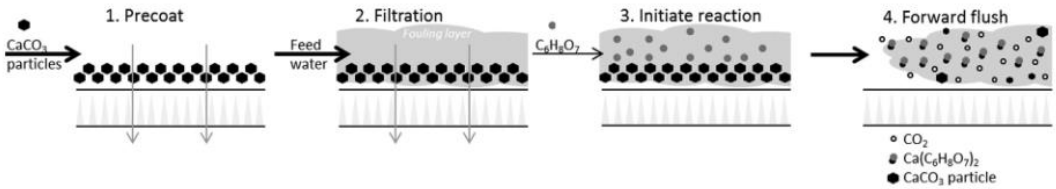

Figure 2.4 Schematic diagram of CaCO3 pre-coating methods (adapted from Kramer et al., 2020): (1) CaCO3 nanoparticles pre-coated on ceramic NF membrane by filtering particle suspension; (2) filtration of sodium alginate as feed water; (3) acid cleaning (citric acid) to initiate the reaction of $CaCO_3$ layer (contaminated by foulants); (4) forward flush to detach and flush away fouling layer.

The stable nanosized particle suspension could be achieved by adjusting the zeta potential. The colloid particle moving under an electric field has a potential at its shear plane, which is defined as zeta potential (Bhattacharjee, 2016). Zeta potential is related to suspension stability. According to DLVO theory, the stability of colloids is determined by the sum of van der Waal's attractive force and electrostatic repulsion force (Duffy et al., 2012). Therefore, the stable suspension could be resulted by making repulsive force exceed attractive force. The increased energy barrier by introducing a charge onto the particle surface could be applied to avoid particle agglomeration. This barrier can be illustrated by the value of zeta potential (Duffy et al., 2012). Generally, the absolute value of zeta potential that exceeds 30 mV indicates a stable system.

Therefore, understanding the zeta potential of $CaCO_3$ helps the preparation of the pre-coating layer. Moulin's study (2003) demonstrated that the potential determining ions

(PDIs) of $CaCO_3$ are calcium ions (Ca^{2+}) and bicarbonate ions (HCO_3^-) that increasing the concentration of PDIs resulted in greater repulsion (Huang et al., 1991; Moulin & Roques, 2003).

2.6 Literature evaluation

The literature review illustrated that municipal sewage reclamation with ceramic NF membrane is viable to alleviate the water shortage worldwide nowadays. The main hurdle to the application of membrane technology is the fouling phenomena during the filtration process. Different prevention and mitigation approaches could be executed according to the types of fouling. While the problematic fouling during wastewater reclamation is organic fouling, and applying $CaCO_3$ pre-coated ceramic NF membrane is regarded as an effective way to prevent the direct interactions between foulants and membrane, restore permeability after acid cleaning, and most importantly, decrease the frequency of NaClO dosing. However, the reaction-based pre-coat methods on ceramic NF membrane completed by Krama is a preliminary study, and the effect of bubbles (reactions shown in Eq. 1.1-1.3) remained unknown. Moreover, the mechanism of the different results obtained from different acid cleaning is unclear. Besides, the maximum effective duration of this method before NaClO cleaning needs to be identified.

3. Materials and methods

3.1 Materials preparation and membrane

3.1.1 Membrane characteristics

In this experiment, multi-channel and single-channel ceramic nanofiltration membranes with titanium dioxide as an active layer produced by Inoper GmbH (Germany) were used. According to the manufacturer, the pore size of the membranes is 0.9 nm and the molecular weight cut-off is 450 Da. The porosity of the membrane is 30-40% and the effective filtration area is 0.1045 m^2. The complete information on the applied ceramic NF membrane is illustrated in Table 3.1. The filtration-cleaning experiments were implemented with the large membrane and the small membrane was applied to determine the thickness of the pre-coating layer.

Table 3.1 specification of the ceramic nanofiltration membrane (Inoper GmbH)

Parameters	Unit	Value
Membrane material	-	TiO_2
Pore size	nm	0.9
Molecular weight cut-off	Da	450
Porosity	%	30-40
Channels	number	19
Outer diameter	mm	25.0
Channel diameter	mm	3
Specific membrane area	m2/m	0.209
Effective membrane area at 0.5m length	m2	0.1045

3.1.2 Preparation of model sewage

To simulate organic foulant in municipal sewage, sodium alginate ($C_6H_9NaO_7$) was used as feed water in the fouling step. Sodium alginate (SA) solution was stirred with a magnetic stirrer for three hours to make it fully dissolved in demi water. As mentioned before, the presence of calcium ions would promote the gel layer formation of sodium alginate, thus calcium chloride ($CaCl_2$, Sigma-Aldrich) was added to the sodium alginate solution. Besides, sodium chloride (NaCl, ≥99.5%, Sigma-Aldrich) and

sodium bicarbonate ($NaHCO_3$, J.T. Baker) were also added to the model sewage solution as a base solution and provided buffering properties to keep pH at 7. The exact concentration of the synthetic sewage is listed in Table 3.2.

3.1.3 Particle suspension

- Calcium carbonate particle suspension

400mg/L of calcium carbonate ($CaCO_3$) suspension was prepared from the reaction (Eq. 3.1) between calcium chloride ($CaCl_2$, Sigma-Aldrich) and sodium bicarbonate ($NaHCO_3$, J.T. Baker). According to Moulin and Roques (2003), the potential determining ions of calcium carbonate are calcium ions and bicarbonate ions, hence extra amounts of calcium chloride ($CaCl_2$, Sigma-Aldrich) and sodium bicarbonate ($NaHCO_3$, J.T. Baker) were added to 4 L of demi water as a base solution to increase the zeta potential (Malvern zetasizer, measured at IHE, Delft) of $CaCO_3$ particle suspension and make it stable. Table 3.2 displays the concentration of the components. 2% hydrochloric acid (HCl, Honeywell Fluka) was added to the $CaCO_3$ suspension to keep the pH at 7.5.

$$2NaHCO_3 + CaCl_2 \rightarrow CaCO_3 + NaCl \quad (3.1)$$

- Calcium hydrogen phosphate particle suspension

400mg/L of calcium hydrogen phosphate ($CaHPO_4$) solution was obtained by mixing calcium chloride ($CaCl_2$, Sigma-Aldrich) and disodium phosphate (Na_2HPO_4, Sigma-Aldrich), and the reaction is shown in Equation 3.2. Extra Na_2HPO_4 (Sigma-Aldrich) was added to 4L demi water as a base solution to increase the absolute value of zeta potential of $CaHPO_4$. Besides, the $CaHPO_4$ suspension was sonicated for 2 hours with ultrasonic cleaner (DK Sonic, China) to keep the particles dispersed and prevent large particle agglomeration. After that, the supernatant of the solution was applied as the feed solution in pre-coating step. Sodium hydroxide solution (NaOH, 5%, Sigma-Aldrich) was used to adjust the pH of $CaHPO_4$ suspension to 7.5.

$$Na_2HPO_4 + CaCl_2 \rightarrow CaHPO_4 + 2NaCl \quad (3.2)$$

The particle size of the pre-coating layer was measured with PSD (Bluewave, Microstrac, USA).

Table 3.2 Materials specification

Compounds	Unit	Value
Synthetic sewage		
Sodium alginate	g/L	0.4
NaCl	mM	5
$CaCl_2$	mM	3
$NaHCO_3$	mM	1
$CaCO_3$ particle suspension		
$CaCl_2$ (for $CaCO_3$ synthesis)	mM	4
$NaHCO_3$ (for $CaCO_3$ synthesis)	mM	8
$CaCl_2$ (base solution)	mM	9
$NaHCO_3$ (base solution)	mM	7.5
pH	-	7.5
$CaHPO_4$ particle suspension		
$CaCl_2$ (for $CaHPO_4$ preparation)	mM	3
Na_2HPO_4 (for $CaHPO_4$ preparation)	mM	3
Na_2HPO_4 (base solution)	mM	5
pH	-	7.5

3.2 Methods

3.2.1 Experimental set-up

The study was conducted in a laboratory-scale cross-flow filtration system and Figure 3.1 illustrates the overall experimental set-up. The whole set-up mainly contains 1) two pumps: a peristaltic pump to dose demineralized water or synthetic sewage into the system, and a cross-flow pump to adjust cross-flow velocity and implement inner recirculation, thus decreasing total energy consumption; 2) a demineralized water tank; 3) a synthetic sewage tank; 4) a pre-coating tank; 5) an acid tank; 6) NaClO tank; 7) membrane configuration and 8) a computer with PLX-DAQ system for data collection. This experiment was performed under a constant flux of 20 $L\cdot(m^2\cdot h)^{-1}$, unless otherwise

specified. The operational conditions for each step are listed in Table 3.3. The conceptual mechanism of this experiment is depicted in Figure 3.2.

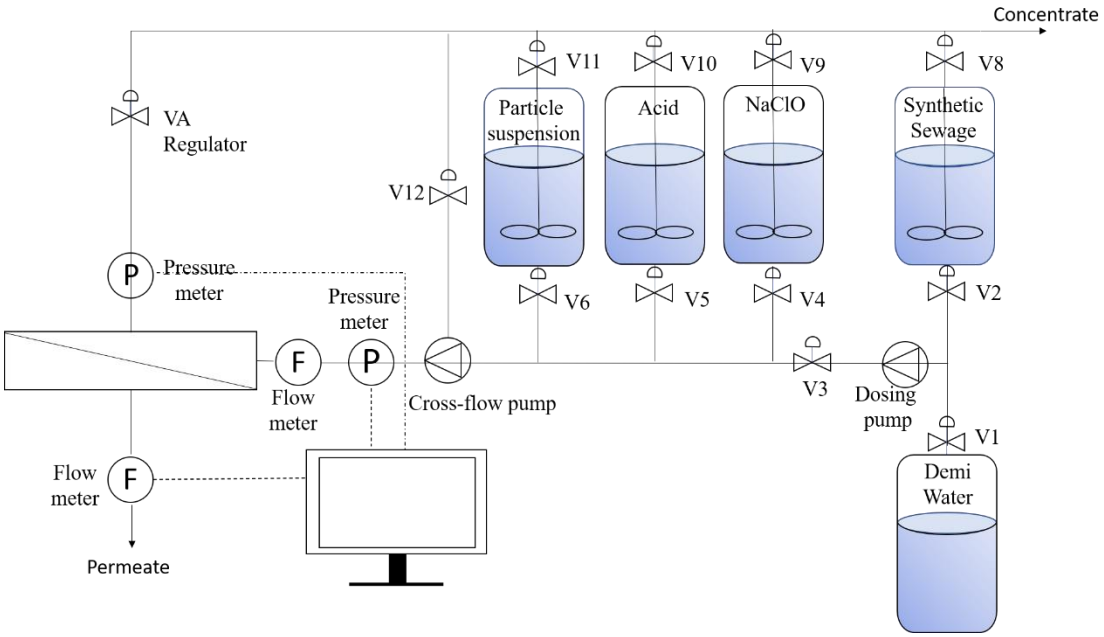

Figure 3.1 Experimental set-up

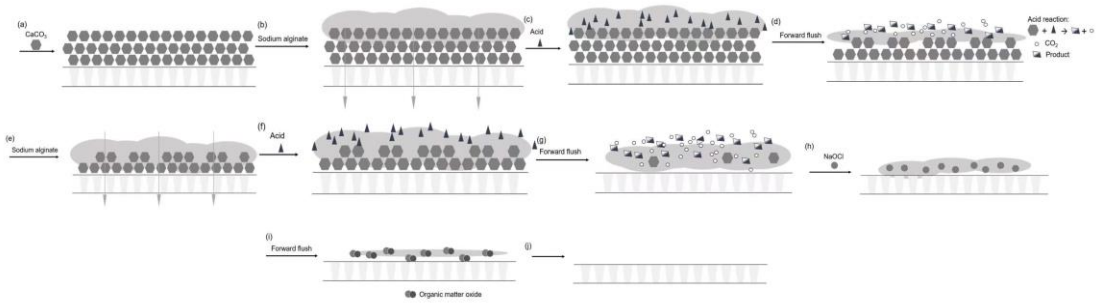

Figure 3.2 Conceptual mechanism of fouling removal with the pre-coated membrane during several filtration/cleaning cycles

3.2.2 Membrane permeability

The membrane permeability before the fouling test and after acid cleaning was determined by a demineralized water filtration test. The cross-flow velocity was 0.32 m/s and valve 12 was opened to implement the inner loop. Membrane permeability was calculated with equation 3.3.

$$L_{20℃} = \frac{J \cdot 9e^{-0.0239(T-20)}}{\Delta P} \qquad (3.3)$$

Where:

$L_{20°C}$: temperature-corrected permeability at 20°C, L·(m^2· h·bar)$^{-1}$;

J: membrane flux, L·(m^2· h)$^{-1}$;

T: temperature of water, °C;

ΔP: transmembrane pressure, bar.

Membrane permeability was normalized that the demi water permeability was set as the baseline (Eq. 3.4). Membrane permeability recovery illustrated the effectiveness of membrane cleaning method and Eq. 3.4 was used to determine the recovery.

$$Normalized\ permeability = \frac{P_i}{P_0} \tag{3.4}$$

$$Recovery = \frac{L_{i,s} - L_{1,e}}{L_{1,s} - L_{1,e}} \tag{3.5}$$

Where:

P_i: permeability of SA filtration in cycle i, L·(m^2· h·bar)$^{-1}$;

P_0: permeability of demi water filtration, L·(m^2· h·bar)$^{-1}$;

$L_{1,s}$: initial permeability in cycle 1, L·(m^2· h·bar)$^{-1}$;

$L_{1,e}$: final permeability in cycle 1, L·(m^2· h·bar)$^{-1}$;

$L_{i,s}$: initial permeability in cycle i, L·(m^2· h·bar)$^{-1}$;

$L_{i,e}$: final permeability in cycle i, L·(m^2· h·bar)$^{-1}$.

3.2.3 Pre-coating method

To ensure the uniform distribution of the attached pre-coating layer, the dead-end mode was performed in this step. The particle suspension was filtrated with the flux of 37 L·(m^2· h)$^{-1}$ under the pressure of eight bar for 10 minutes. SEM (FEI, USA) analysis was performed on the pre-coated small single-channel membrane to determine the thickness of the effective pre-coating layer. This process was only executed before the first fouling test, which was not repeated in the following cycles.

3.2.4 Fouling test

Synthetic sewage was filtrated in a large membrane configuration with a cross-flow velocity of 0.32 m/s with a duration of 40 min, which is about five days in reality. The retentate was recirculated to the feed synthetic sewage tank and an inner loop was conducted with valve 12 opened.

3.2.5 Acid cleaning

Three different acids were applied here to compare the effect of acid cleaning and to initiate the reaction between the pre-coating layer and acids, which are 1g/L hydrochloric acid (HCl, Honeywell Fluka), 1g/L formic acid (CH_2O_2, Sigma-Aldrich) and 1g/L citric acid ($C_6H_8O_7$, Merk KGaA). The reactions between $CaCO_3$ and three acids (Eq. 3.4-3.7) could generate calcium carbonate (CO_2) bubbles while the reactions between $CaHPO_4$ and acids do not initiate bubbles release (Eq 3.8).

$$CaCO_3(s) + 2H^+ \rightarrow Ca^{2+} + H_2O + CO_2(g) \quad (3.4)$$

$$CaCO_3(s) + 2HCOOH(aq) \rightarrow Ca(COO)_2(aq) + 2H^+ + CO_3^{2-} \quad (3.5)$$

$$3CaCO_3(s) + 2(CH_2COOH)_2C(OH)COOH(aq) \rightarrow Ca_3((CH_2COO)_2C(OH)COO)_2(aq) + 6H^+ + 3CO_3^{2-} \quad (3.6)$$

$$H_2CO_3(aq) \rightarrow H_2O + CO_2(g) \quad (3.7)$$

$$3CaHPO_4(s) + 2(CH_2COOH)_2C(OH)COOH(aq) \rightarrow Ca_3((CH_2COO)_2C(OH)COO)_2(aq) + H_3PO_4(aq) \quad (3.8)$$

Reaction-based acid cleaning was operated with the cross-flow velocity of 0.1 m/s for 10 min. The regulator valve (VA) was adjusted so that there was no permeate through the membrane and the generated concentrate was recirculated into the acid tank. After each acid cleaning, 10mL of samples were collected from the acid tank to determine the concentration of calcium ions with IC analysis (Metrohm, Netherlands), which

represents the consumed pre-coating layer.

3.2.6 Forward flush

Acid cleaning was followed by forward flush and VA was completely opened (hence no permeate). Forward flush was operated with demineralized water at 0.5 m/s for 10 min.

3.2.7 Sodium hypochlorite cleaning

Section 3.2.2-3.2.6 completes one cycle (Section 3.2.3 was only executed in the first cycle). After 3 or 6 cycles, 0.1% sodium hypochlorite (NaClO, Boom) was used for thoroughly cleaning and irreversible foulants removal. NaClO cleaning was conducted at a cross-flow velocity of 0.1 m/s for an hour with VA opened, and the retentate was recirculated.

Table 3.3 Experimental operating conditions

Step	Applied pump	Opened valve	Cross-flow velocity (m/s)	Permeate flux (L·(m^2·h)$^{-1}$)
Membrane permeability	Dosing pump & cross-flow pump	V1, V3, V12 VA (regulating),	0.32	20
Pre-coating	Cross-flow pump	V6, V11	-	37
Fouling test	Dosing pump & cross-flow pump	V2, V3, V8, V12, VA (regulating),	0.32	20
Acid cleaning	Cross-flow pump	V5, V10, VA (completely opened)	0.1	0
Forward flush	Cross-flow pump	V1, V3, VA (completely opened)	0.5	0
NaClO cleaning	Cross-flow pump	V4, V9, VA (completely opened)	0.1	0

4. Results & Discussions

4.1 Comparison between pristine membranes and $CaCO_3$ pre-coated membranes

Three preliminary tests were implemented to test the effectiveness of calcium carbonate pre-coated membranes. One filtration/acid cleaning cycle was applied in the preliminary experiments. Firstly, the fouling curve of the pristine membranes and pre-coated membranes were compared. It can be seen from Figure 4.1 that the fouling curves of the pre-coated membranes are similar to that of the clean membranes. The fouling curves of the pristine membranes ended at slightly slower points than pre-coated membranes after 40 minutes of filtration. Secondly, the impacts of three different acids: citric acid (Figure 4.1a), formic acid (Figure 4.1b) and hydrochloric acid (Figure 4.1c), on pristine membranes and pre-coated membranes were determined. The permeability of the uncoated membrane cleaned with citric acid witnessed an increase of 18% while the permeability of the coated membrane was increased to 86% (Figure 4.1a). The untreated membrane after formic acid cleaning showed a growth of 30% in permeability but the permeability of the pre-coated membrane rose to 76% (Figure 4.1b). Similarly, the permeability recovery of the pre-coated membrane after hydrochloric cleaning (restored to 70%) was about twice that of the pristine membrane (increased to 37%) (Figure 4.1cFigure 3.2). Since the permeability recovery of the pristine membranes was too low, no further comparison between the pristine membrane and the pre-coated membrane in more cycles was needed. These results indicated that the reaction-based pre-coating method was effective for fouling control.

In both pristine membranes and $CaCO_3$ pre-coated membranes, a drop in initial permeability (around 20%) was observed. This phenomenon was consistent with previous research. Garciá-Molina et al. (2006) reported a drop in initial fouling permeability when increasing the concentration of alginic acid foulants and it was attributed to the concentration polarisation caused by the concentrated feed solution. Katsoufidou et al. (2007) investigated the drop of the initial flux of fouling compared with the initial flux of clean membrane with dead-end ultrafiltration membrane and it

was suggested that the drop was caused by the rapid adsorption of sodium alginate at the initial stage.

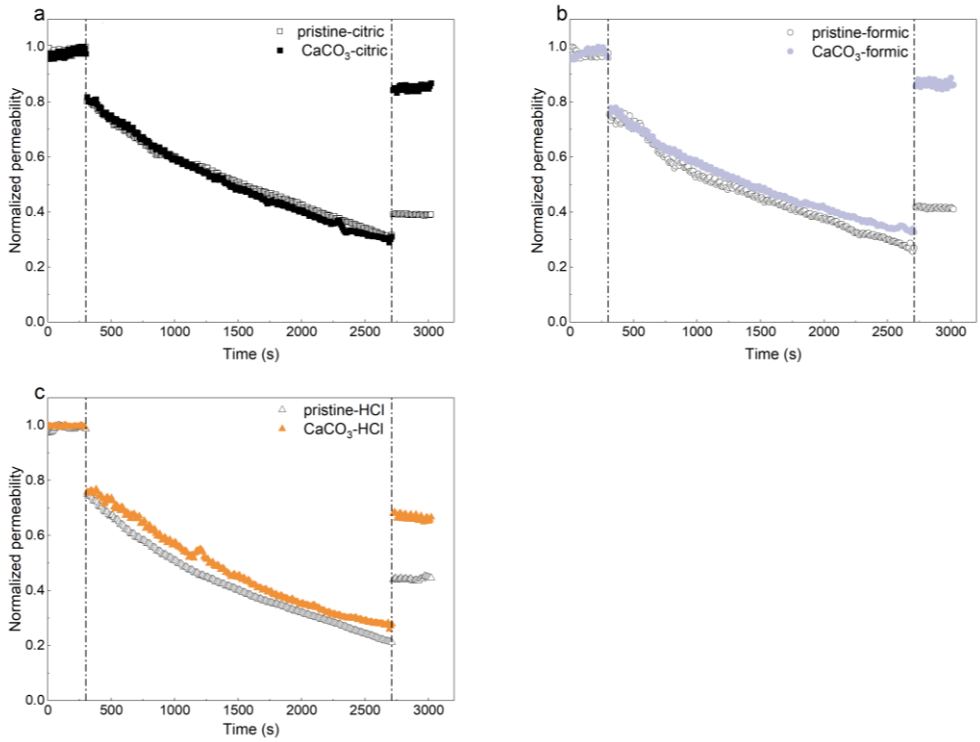

Figure 4.1 Normalized permeability of both the pristine membranes (white) and calcium carbonate pre-coated membranes after (a) citric acid (black) cleaning; (b) formic acid (purple) cleaning; (c) and hydrochloric acid (orange) cleaning.

4.2 Effects of calcium carbonate pre-coated membranes during three cycles

Several experiments with three filtration/acid cleaning cycles were executed to determine the effectiveness of three different acids. The $CaCO_3$ pre-coat was not refreshed between the cycles. Firstly, the characterization of the $CaCO_3$ pre-coated membrane was completed. The average particle size of the $CaCO_3$ suspension was 0.315 μm (Figure 4.6), which is larger than the pore size of the applied ceramic NF membrane (0.9 nm), indicating that $CaCO_3$ could deposit on the membrane surface without entering the pores. As shown in Figure 4.2, $CaCO_3$ particles were successfully deposited on the membrane surface with an average thickness of 7.049 μm.

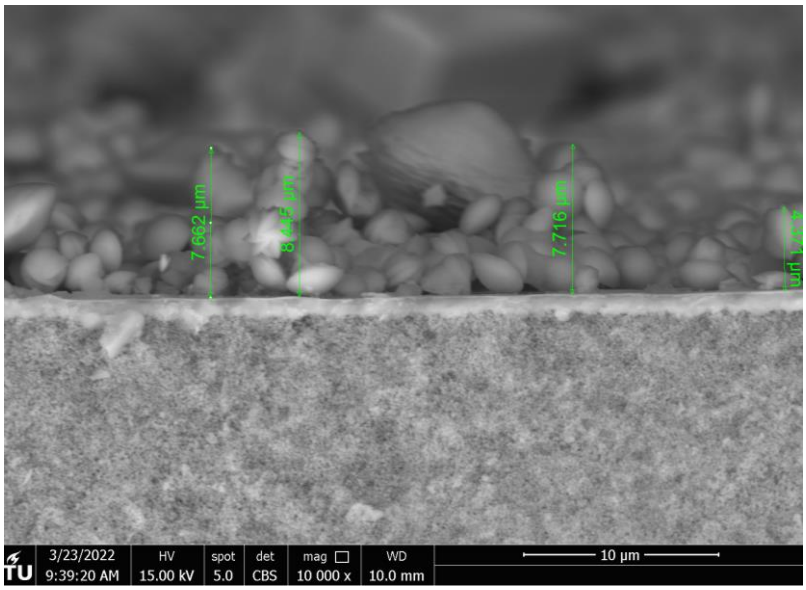

Figure 4.2 The thickness of the $CaCO_3$ layer.

Secondly, the fouling curve and the permeability recovery were compared after different types of acid cleaning (Figure 4.3a). During the first cycle, the fouling curves of the three tests were almost identical while for the hydrochloric acid test, the starting point and end point were slightly lower than the other two. This could be attributed to the preparation of sodium alginate (SA) error. After the first cleaning, the permeability of three acid tests was restored to different extents. Citric acid cleaning performed the highest permeability recovery of 86% and formic ranked second with an increase of 76% (Table 4.1). HCl cleaning showed a lesser effect: permeability rose to about 70% (Table 4.1). Similarly, the effectiveness of citric acid was highest after the second cleaning among the three acids, while the permeability recovery of HCl was not comparable (Table 4.1). According to the permeability recovery extent, the effectiveness of the acids decreases in the order of citric acid, formic acid, HCl. Compared with the previous work by Kramer et al. (2020), similar results were obtained that the permeability recovery after first citric acid cleaning (76%) was higher than that of HCl cleaning (12%). The efficiency of this study was better than Kramer's research mainly because of the optimized higher acid concentration and lower foulants load was applied. Moreover, the second acid cleaning efficiency in this study was much higher than Kramer et al.'s study (2020) (approximately restored to 10%). In his experiment, the

pre-coat was refreshed for the second cycle, and the unremoved SA from the last cycle could affect the deposition of pre-coat layer on the membrane surface.

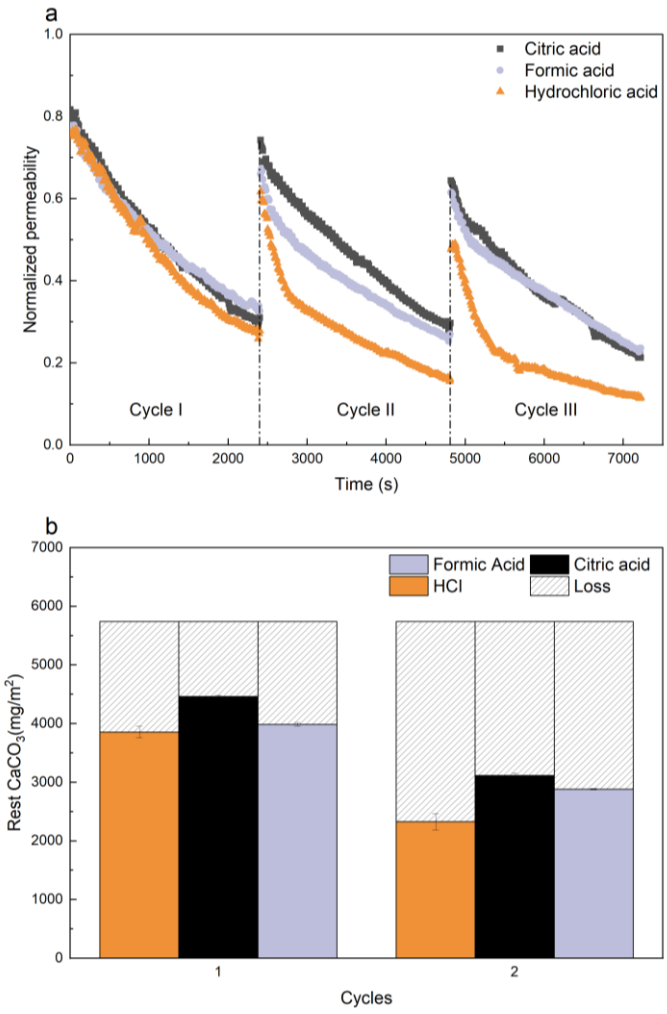

Figure 4.3 Comparison of (a) fouling curves among formic acid (purple), citric acid (black) and HCl (orange) with reaction-based pre-coat using $CaCO_3$ during three cycles; (b)Remaining $CaCO_3$ on the membrane surface.

These differences could be explained by the different reaction mechanisms between the acids and $CaCO_3$. Citric acid is a chelating agent, containing three carboxyl groups (-COOH) and formic acid is a monocarboxylic acid (Figure 4.4a & Figure 4.4b). The deprotonated carboxyl functional groups ($-COO^-$) have a chelation affinity towards calcium ions to produce complex substances (X. Li et al., 2015). Both citric acid and formic acid can dissolve $CaCO_3$, and act as a strong Ca^{2+} entrapment agent, forming calcium citrate chelates and calcium formate complexes when pH >2 (Figure 4.4c & d)

(Ghoorah et al., 2014; Karar et al., 2016; Mitsionis et al., 2010). The above process would assist in the loosening and detachment of the $CaCO_3$--SA layer. Besides, the chelates with larger molecular weight could provide sufficient adsorption sites for SA, therefore more SA was flushed away, contributing to higher permeability recovery after citric acid cleaning. While in the case of HCl, no complexes or chelates were produced to help the detachment of most SA. Additionally, the released Ca^{2+} would probably chelate with SA and bridge the unstrapped SA with the attached SA, contributing to the increased fouling rate.

The reason for the high permeability recovery after citric acid cleaning is also proposed that during the diffusion of citric acid from bulk solution to $CaCO_3$ pre-coating layer, it would entrap the Ca^{2+} from the compact SA layer due to the larger stability constant of calcium citrate complex (Q. Li & Elimelech, 2004; Lin et al., 2021). The integrity of the cross-linked SA layer was therefore destructed and became more easily to be flushed off (Q. Li & Elimelech, 2004).

Table 4.1 Permeability recovery after three acid cleaning methods

Acid cleaning	Citric acid	Formic acid	Hydrochloric acid
First cleaning	86%	76%	70%
Second cleaning	67%	63%	45%

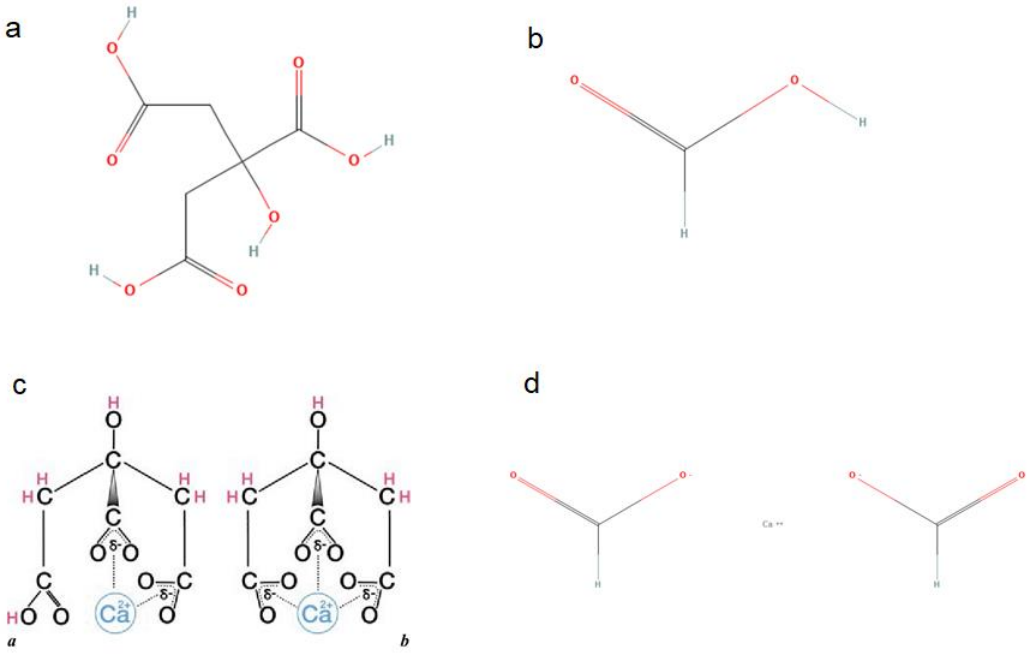

Figure 4.4 Structure of (a) citric acid; (b) formic acid; (c) calcium citrate; and (d) calcium formate. (a), (b) & (d) were adapted from PubChem https://pubchem.ncbi.nlm.nih.gov/compound/311 https://pubchem.ncbi.nlm.nih.gov/compound/284 & https://pubchem.ncbi.nlm.nih.gov/compound/10997 and (c) was adapted from https://www.researchgate.net/figure/Schematic-representation-of-citrate-ion-chelating-a-calcium-ion-The-diagram-represent_fig20_7093259

In the second and third cycles, there was a pronounced difference among these fouling curves. At the initial stage of fouling, the permeability of the pre-coated membrane after the first HCl cleaning dropped dramatically. This phenomenon could be explained by the unevenly dissolved $CaCO_3$ pre-coat layer by HCl. Therefore, some part of the pristine membrane was exposed to the SA while other part was still covered by the pre-coat layer, resulting in uneven distribution of flux. When the next filtration started, the flux at the clean membrane surface was higher than that at pre-coated area at constant flux operation condition. Consequently, the SA layer built up was accelerated at clean area until the flux was restored to the even distribution on the membrane surface. This could also be ascribed to the low effectiveness of HCl cleaning that more SA remained

on the membrane. The increased concentration of SA was responsible for the abrupt drop in permeability in the second run (Zazouli et al., 2010). Afterwards, a smooth decrease in permeability was detected, indicating the formation of the cake filtration layer (Lin et al., 2021). The endpoints of the HCl cleaning group were much lower than the other groups. It is considered to be caused by the strong intermolecular interactions with excess SA by hydrogen bonding with their hydroxyl groups, followed by a thicker SA layer formation (Hashino et al., 2011).

The consumption of the $CaCO_3$ layer for the three tests is depicted in Figure 4.3b. During the first and the second cleaning, more $CaCO_3$ was reacted with the strong acid HCl, while the least was consumed with citric acid. Therefore, during the whole process, a relatively thicker $CaCO_3$ pre-coating layer remained in the citric acid cleaning group, protecting the ceramic NF membrane. In the case of HCl cleaning, because more $CaCO_3$ was dissolved with HCl, in addition to the forward flush, the pre-coating layer could not be uniformly distributed on the membrane surface. As a result, the ceramic NF membrane could be directly exposed to SA and severe fouling occurred.

4.3 Reaction-based $CaCO_3$ pre-coat with multiple cycles

To test the performances of three acid cleaning on pre-coated membranes for longer-term usage, several experiments were conducted for six cycles with 7655 mg/m^2 $CaCO_3$ deposited on the membranes. The $CaCO_3$ pre-coat was not refreshed during the whole process. The results obtained (Figure 4.4) were similar to those from three cycles.

Firstly, the feasibility of applying six cycles on the pre-coated membranes with different acid cleaning was compared (Figure 4.5a). From the fourth cycle, $CaCO_3$ pre-coated membrane with HCl cleaning got fouled quickly and could not complete the filtration test (40 min). Therefore, $CaCO_3$ pre-coating/HCl cleaning showed a marginal effect on long-term application. Pre-coated membrane cleaned with formic acid could barely maintain six cycles and the pre-treated membrane executed with citric acid cleaning

showed considerable effectiveness during six fouling cycles.

Secondly, the fouling curve and permeability recovery were analyzed. In the first cycle, the fouling curve trends of the three groups were comparable. The starting point of the $CaCO_3$/HCl group was marginally higher than the other two. A possible reason could be the error in the preparation of the foulants. In cycle II and III, a drastic drop in permeability of the $CaCO_3$/HCl group was observed and the reason was illustrated in Sec.4.1.

The overall permeability restoration decreases in the order of citric acid, formic acid and then hydrochloric acid (Table 4.2). As shown in Table 4.2, most of the permeability (> 88%) was maintained after the first two citric acid cleaning. Notwithstanding, the permeability recovery of $CaCO_3$/citric acid from the last cycle decreased dramatically compared with the former ones, though enough $CaCO_3$ remained on the membrane (Figure 4.5b). This was possibly resulted from the partial membrane surface exposure to SA due to the uneven distribution of the pre-coating layer after several times of filtration and cleaning.

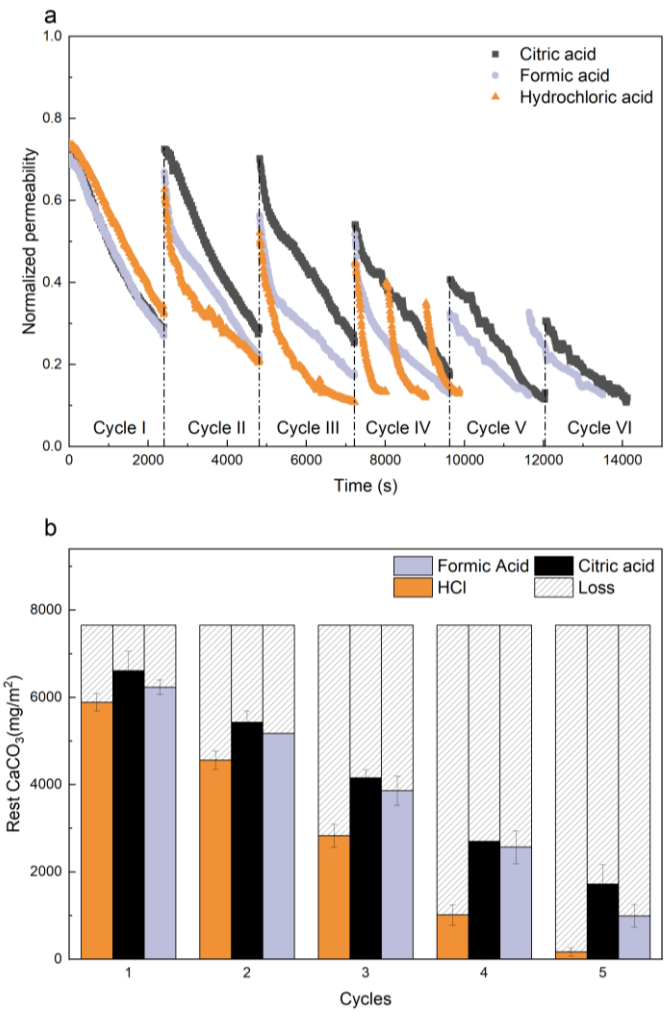

Figure 4.5. Comparison of (a) fouling curves among three acids with reaction-based pre-coat using $CaCO_3$ during three cycles; (b) Remaining $CaCO_3$ on the membrane surface.

Figure 4.5b compares the remaining $CaCO_3$ on the membranes for different tests. Half of the pre-coating layer was removed after three times of HCl cleaning and almost no effective protective layers was left on the membranes at the end. This could explain the quick fouling after Cycle III for $CaCO_3$/HCl test. It is apparent that the amount of remaining effective pre-coating layer for the $CaCO_3$/citric test was the highest. This result confirms the highest permeability recovery after citric cleaning for six cycles, which is equal to 30 days in real application (Kramer et al., 2020).

Table 4.2 Permeability recovery after three acid cleaning methods for 6 cycles

Acid cleaning	Citric acid	Formic acid	Hydrochloric acid

First cleaning	95%	82%	76%
Second cleaning	88%	68%	48%
Third cleaning	58%	57%	31%
Fourth cleaning	30%	13%	19%
Fifth cleaning	9%	12%	6%

4.4 Effects of bubbles

To further detect the influence of bubbles on fouling removal, $CaHPO_4$, which did not generate bubbles during the reaction with acids, was applied as the pre-coating layer as a control group. At first, $Ca_3(PO_4)_2$ was selected as the control group, but the molecular weight of it is too large (310.18 g/mol), so $CaHPO_4$, whose molecular weight (136.06 g/mol) was closer to that of $CaCO_3$ (100.09 g/mol), was used instead.

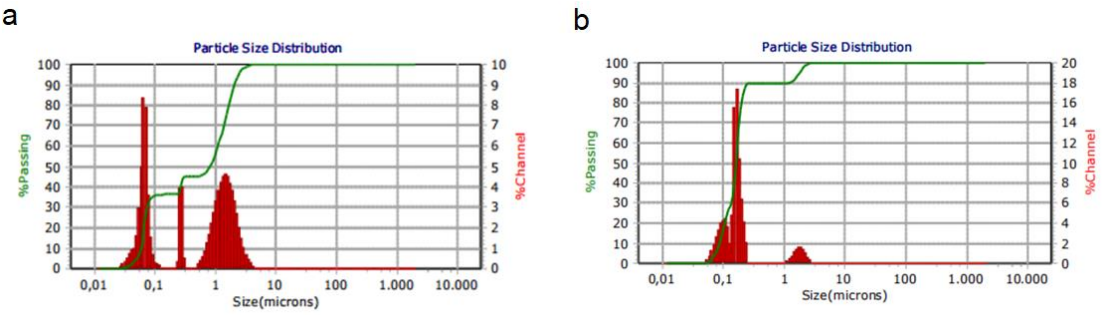

Figure 4.6 Particle size distribution of (a) $CaHPO_4$ particle suspension (mean size: 0.886 μm) and (b) $CaCO_3$ particle suspension (mean size: 0.315 μm)

To begin with, the effect of $CaHPO_4$ pre-coating with citric acid cleaning was compared with the pristine membrane and the $CaCO_3$ pre-coated membrane. $CaHPO_4$ pre-coated membrane exhibited a more severe fouling extent that the endpoint of the fouling curve was lower than that of the pristine and $CaCO_3$ pre-coated membranes (Figure 4.7). As shown in Figure 4.6, the particle size of the $CaHPO_4$ suspension (0.886 μm) was larger than the $CaCO_3$ suspension (0.315 μm), hence the channels of the $CaHPO_4$ layer could be wider than $CaCO_3$ layer; or more porous. SA foulants could pass through the pores, therefore fouled the membrane. Additionally, the solubility of $CaHPO_4$ ($K_{sp} = 1 \times 10^{-7}$) is higher than $CaCO_3$ ($K_{sp} = 2.8 \times 10^{-9}$) at room temperature and probably the deposited $CaHPO_4$ generated free Ca^{2+} which increased the viscosity of

SA, leading to more severe fouling (Xie et al., 2003). A more drastic decline and more severe fouling rate were also detected by Garciá-Molina et al. (2006) with the increased concentration of Ca^{2+} when filtering alginic acid with UF membranes. The partial dissolution of $CaHPO_4$ may result in the uneven distribution of the pre-coating layer.

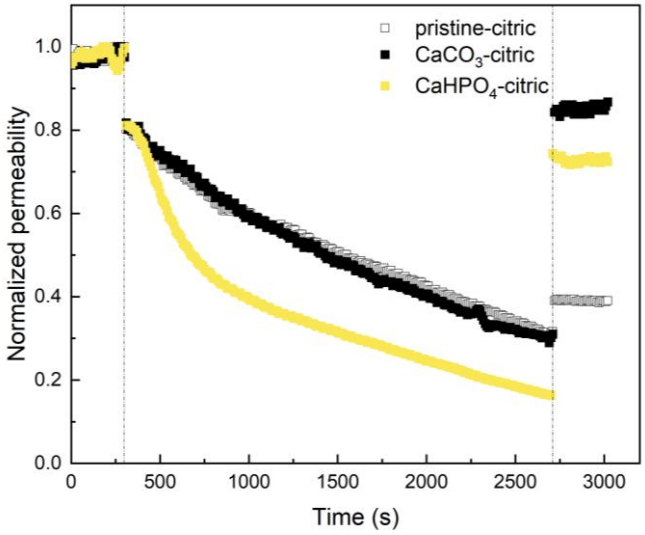

Figure 4.7 Effectiveness of $CaHPO_4$ (yellow) pre-coated membrane compared with the pristine (white) membrane and the $CaCO_3$ (black) pre-coated membrane

Then, the experiment performing three filtration/cleaning cycles without refreshing $CaHPO_4$ was conducted. The results are shown in Figure 4.8.

As illustrated before, in the first filtration/cleaning cycle, the fouling phenomenon of the $CaHPO_4$ pre-coated membrane was more serious than the $CaCO_3$ pre-coated membrane. Figure 4.8a displays the fouling curve of the two pre-coated membranes. A pronounced disparity between the control groups was discovered. After the first citric acid cleaning, the permeability of the $CaHPO_4$ pre-coated membrane was restored to 66% (Table 4.3), which was lower than the permeability recovery after the second cleaning for the $CaCO_3$ pre-coated membrane. One speculation was proposed that the released Ca^{2+} from $CaHPO_4$ caused the enhanced gelation of sodium alginate, therefore the difficulty of loosening SA could rise. The remaining SA from the last cycle and the foulants from the new cycle could cause the sharp decline of permeability. The increased concentration of Ca^{2+} in the bulk solution may contribute to a denser and

more compact gel layer, increasing the difficulty of the diffusion of citric acid (Ang et al., 2006). As a result, the cleaning efficiency of citric acid was possibly decreased hence $CaHPO_4$ pre-coated membrane showed a lower permeability recovery than $CaCO_3$ pre-coated membrane.

With respect to the pre-coating layer consumption during acid cleaning (Figure 4.8b), the pre-coating layer consumptions after the first citric acid cleaning for both control groups were comparable. However, the permeability recovery of $CaHPO_4$ pre-coated membrane was lower than $CaCO_3$ pre-coated membrane.

Recapitulating, it is hard to conclude that the higher permeability recovery of $CaCO_3$ pre-coated membrane was the consequence of the positive impact of bubbles because the reaction kinetics between citric acids and $CaHPO_4$ could be different from $CaCO_3$. Moreover, the different solubility of these two solids would contribute to the different fouling phenomena. Besides, it is interesting to find that though the fouling on CaHPO4 pre-coated membrane was more severe than CaCO3 pre-coated membrane, the cleaning efficiencies of them were not too different (Figure 4.8). Section 4.2 & 4.3 show that more $CaCO_3$ was reacted when cleaned with HCl, indicating more bubbles were generated. However, HCl cleaning was the least efficient chemical agent to remove SA on $CaCO_3$ pre-coated ceramic NF membranes.

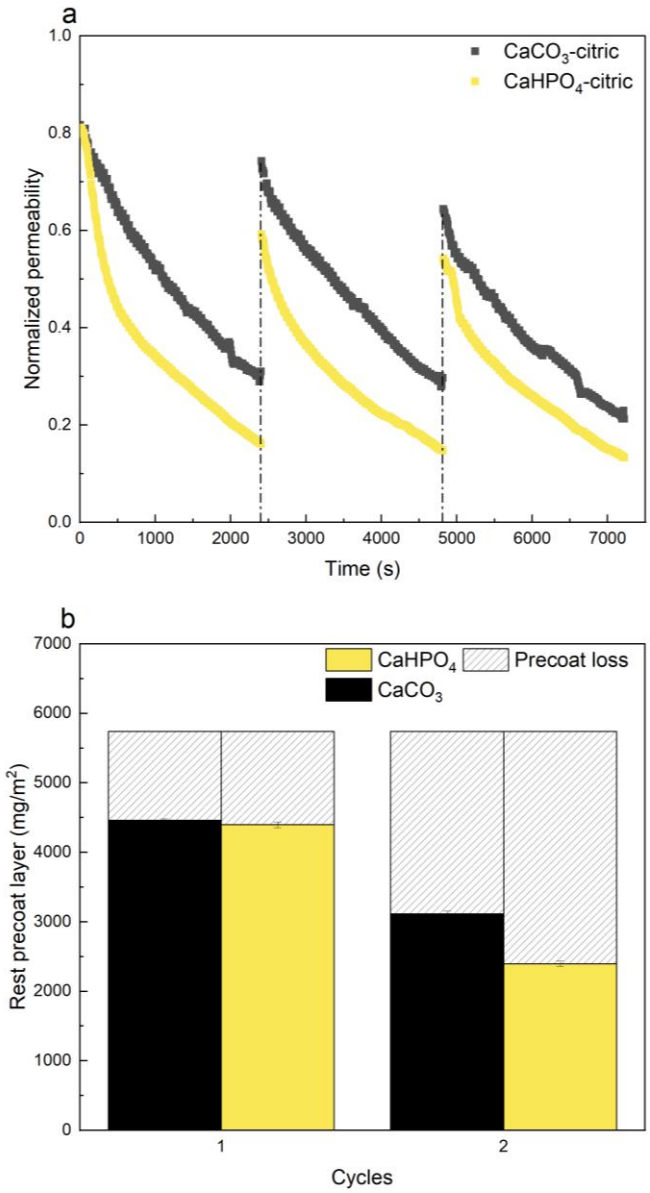

Figure 4.8 Comparison of (a) fouling curves between $CaCO_3$ pre-coated membrane (black) and $CaHPO_4$ pre-coated membrane (yellow) applying citric acid cleaning during three cycles; (b) Remaining $CaCO_3$ (black)/$CaHPO_4$ (yellow) on the membrane surface

Table 4.3 Permeability recovery of $CaCO_3$ pre-coated membrane and $CaHPO_4$ pre-coated membrane after citric acid cleaning

Acid cleaning	$CaCO_3$ pre-coat	$CaHPO_4$ pre-coat
First cleaning	86%	66%
Second cleaning	67%	58%

5. Conclusions

The major goal of this study is to evaluate the effectiveness of different acid cleaning on $CaCO_3$ pre-coated membranes. And the feasibility of applying more filtration/cleaning cycles was explored. Finally, the impact of bubbles on fouling control was investigated.

The research questions could be answered as bellows:

1. What is the effect of different acid cleaning (formic acid, citric acid, and hydrochloric acid)?

   During both short-term (three filtration/acid cleaning cycles) and long-term (six filtration/acid cleaning cycles) experiments, citric acid cleaning efficiency prevails over other acids because of the relatively moderate reaction and chelated formation; formic acid showed moderate foulant removal efficiency and the permeability recovery of HCl cleaning was the lowest. For HCl cleaning, after the first filtration/cleaning cycle, the fouling at initial stage of the next cycles was severe due to the uneven dissolving of $CaCO_3$ pre-coat layer.

2. How many effective cycles can last for the pre-coating fouling test?

   Six filtration/acid cleaning cycles were executed. The result demonstrated that HCl consumed a large amount of $CaCO_3$ that after the third cycle the permeability of the membrane dropped sharply and could not last for 40 min (one filtration cycle = 40 min). Pre-coated membrane cleaned with formic acid could barely complete six cycles (30 days in reality). Citric acid cleaning for the pre-coated membrane exhibited the greatest fouling control properties that there was approximately a quarter of $CaCO_3$ on the membrane.

3. What is the influence of carbon dioxide bubbles during the acid cleaning process?

The $CaCO_3$ pre-coated membrane with citric acid cleaning was compared with the $CaHPO_4$ pre-coated membrane. It is found that the fouling phenomenon was more severe than $CaCO_3$ which could be attributing to the larger and more porous CaHPO4 layer. Interestingly, the cleaning efficiencies did not differ a lot, so the impact of bubbles may not be significant.

6. Recommendations

Some preliminary conclusions were obtained in this study. $CaCO_3$ pre-coated membrane with citric acid cleaning manifested promising effectiveness on organic fouling control on ceramic NF membranes. However, there are still some limitations.

The combined model sewage foulants could be conducted on the $CaCO_3$ pre-coated membrane to measure the efficiency of citric acid cleaning methods. Municipal sewage contains more than one single foulants like SA, therefore, humic acids (HA), bovine serum albumin (BSA) along with SA could be applied as combined surrogate foulants in the municipal sewage. There were some researches exploring the synergetic effect of the above foulants and the fouling rate would be increased when filtering mixtures of organic foulants (de Angelis & de Cortalezzi, 2013; Zazouli et al., 2010). If possible, municipal sewage could be directly applied to test the viability of reaction-based $CaCO_3$ pre-coating with acid cleaning. Additionally, calcium silicate ($CaSiO_3$) could be selected as an alternative of $CaHPO_4$ to explore the exact impact of bubbles. Calcium silicate did no generate CO_2 during the reaction with acids and it may perform smaller particles size thus may display similar fouling curve trend as the $CaCO_3$ pre-coated membrane.

It was found that $CaCO_3$ pre-coated membrane could work for six filtration/citric acid cleaning cycles before NaClO dosing to remove all foulants. This finding is meaningful in reality since six cycles equal to 30 days (Kramer et al., 2020). Therefore, if the reaction-based pre-coating with $CaCO_3$ could be scaled up to the real application, then the frequency of NaClO dosing could be broadly decreased, therefore the longevity of ceramic NF membranes could be maintained. The feasibility of dosing a thicker layer of $CaCO_3$ to maintain more effective cycles could be investigated in the future.

References

Al-Malack, M. H., & Anderson, G. K. (1998). Use of chemical species as dynamic membranes with crossflow microfiltration. *Separation Science and Technology*, *33*(16), 2491–2511. https://doi.org/10.1080/01496399808545315

Amy, G. (2008). Fundamental understanding of organic matter fouling of membranes. *Desalination*, *231*(1–3), 44–51. https://doi.org/10.1016/j.desal.2007.11.037

Anantharaman, A., Chun, Y., Hua, T., Chew, J. W., & Wang, R. (2020). Pre-deposited dynamic membrane filtration – A review. In *Water Research* (Vol. 173). Elsevier Ltd. https://doi.org/10.1016/j.watres.2020.115558

Ang, W. S., Lee, S., & Elimelech, M. (2006). Chemical and physical aspects of cleaning of organic-fouled reverse osmosis membranes. *Journal of Membrane Science*, *272*(1–2), 198–210. https://doi.org/10.1016/j.memsci.2005.07.035

Arumugham, T., Kaleekkal, N. J., Gopal, S., Nambikkattu, J., K, R., Aboulella, A. M., Ranil Wickramasinghe, S., & Banat, F. (2021). Recent developments in porous ceramic membranes for wastewater treatment and desalination: A review. In *Journal of Environmental Management* (Vol. 293). Academic Press. https://doi.org/10.1016/j.jenvman.2021.112925

Asif, M. B., & Zhang, Z. (2021). Ceramic membrane technology for water and wastewater treatment: A critical review of performance, full-scale applications, membrane fouling and prospects. *Chemical Engineering Journal*, *418*. https://doi.org/10.1016/j.cej.2021.129481

Benfer, S., Árki, P., & Tomandl, G. (2004). Ceramic Membranes for Filtration Applications — Preparation and Characterization. *Advanced Engineering Materials*, *6*(7), 495–500. https://doi.org/10.1002/adem.200400577

Bhattacharjee, S. (2016). DLS and zeta potential - What they are and what they are not? *Journal of Controlled Release*, *235*, 337–351. https://doi.org/10.1016/j.jconrel.2016.06.017

Chen, J. P., Kim, S. L., & Ting, Y. P. (2003). Optimization of membrane physical and chemical cleaning by a statistically designed approach. *Journal of Membrane Science*, *219*(1–2), 27–45. https://doi.org/10.1016/S0376-7388(03)00174-1

Combe, C., Guizard, C., Aamar ', E., & Sanchez, V. (1997). Experimental determination of four characteristics used to predict the retention of a ceramic nanofiltration membrane. In *Journal of Membrane Science* (Vol. 129).

de Angelis, L., & de Cortalezzi, M. M. F. (2013). Ceramic membrane filtration of organic compounds: Effect of concentration, pH, and mixtures interactions on fouling. *Separation and Purification Technology*, *118*, 762–775. https://doi.org/10.1016/j.seppur.2013.08.016

Duffy, J. J., Panalytical, M., & Hill, A. J. (2012). Suspension Stability; Why Particle Size, Zeta Potential and Rheology are Important. *Annual Transactions of the Nordic Rheology Society*, *20*(2012), 6. https://www.researchgate.net/publication/279851764

Galjaard, G., Buijs, P., Beerendonk, E., Schoonenberg, F., & Schippers, J. Ç. (2001). Pre-coating (EPCE®) UF membranes for direct treatment of surface water. *Desalination*, *139*(1–3), 305–316. https://doi.org/10.1016/S0011-9164(01)00324-1

Galjaard, G., Kruithof, J. C., Scheerman, H., Verdouw, J., & Schippers, J. C. (2003). Enhanced pre-coat engineering (EPCE ®) for micro-and ultrafiltration: steps to full-scale application. *Water Science and Technology: Water Supply*, *3*(5–6), 125–132.

http://iwaponline.com/ws/article-pdf/3/5-6/125/419266/125.pdf

Galjaard, G., van Paassen, J., Buijs, P., & Schoonenberg, F. (2001). Enhanced pre-coat engineering (EPCE) for micro-and ultrafiltration: the solution for fouling? *Water Science and Technology: Water Supply*, *1*(5–6), 151–156. http://iwaponline.com/ws/article-pdf/1/5-6/151/477265/151.pdf

Gao, B., Liu, L., Liu, J., & Yang, F. (2013). A photo-catalysis and rotating nano-CaCO3 dynamic membrane system with Fe-ZnIn2S4 efficiently removes halogenated compounds in water. *Applied Catalysis B: Environmental*, *138–139*, 62–69. https://doi.org/10.1016/J.APCATB.2013.02.023

Gao, W., Liang, H., Ma, J., Han, M., Chen, Z. lin, Han, Z. shuang, & Li, G. bai. (2011). Membrane fouling control in ultrafiltration technology for drinking water production: A review. *Desalination*, *272*(1–3), 1–8. https://doi.org/10.1016/J.DESAL.2011.01.051

Garciá-Molina, V., Lyko, S., Esplugas, S., Wintgens, T., & Melin, T. (2006). Ultrafiltration of aqueous solutions containing organic polymers. *Desalination*, *189*(1-3 SPEC. ISS.), 110–118. https://doi.org/10.1016/j.desal.2005.11.002

Ghoorah, M., Dlugogorski, B. Z., Balucan, R. D., & Kennedy, E. M. (2014). Selection of acid for weak acid processing of wollastonite for mineralisation of CO2. *Fuel*, *122*, 277–286. https://doi.org/10.1016/j.fuel.2014.01.015

Goh, P. S., Lau, W. J., Othman, M. H. D., & Ismail, A. F. (2018). Membrane fouling in desalination and its mitigation strategies. *Desalination*, *425*, 130–155. https://doi.org/10.1016/J.DESAL.2017.10.018

Griffiths, I. M., Kumar, A., & Stewart, P. S. (2014). A combined network model for membrane fouling. *Journal of Colloid and Interface Science*, *432*, 10–18. https://doi.org/10.1016/j.jcis.2014.06.021

Gude, V. G. (2017). Desalination and water reuse to address global water scarcity. *Reviews in Environmental Science and Biotechnology*, *16*(4), 591–609. https://doi.org/10.1007/S11157-017-9449-7

Guo, W., Ngo, H. H., & Li, J. (2012). A mini-review on membrane fouling. *Bioresource Technology*, *122*, 27–34. https://doi.org/10.1016/J.BIORTECH.2012.04.089

Hashino, M., Hirami, K., Katagiri, T., Kubota, N., Ohmukai, Y., Ishigami, T., Maruyama, T., & Matsuyama, H. (2011). Effects of three natural organic matter types on cellulose acetate butyrate microfiltration membrane fouling. *Journal of Membrane Science*, *379*(1–2), 233–238. https://doi.org/10.1016/j.memsci.2011.05.068

Hofs, B., Ogier, J., Vries, D., Beerendonk, E. F., & Cornelissen, E. R. (2011). Comparison of ceramic and polymeric membrane permeability and fouling using surface water. *Separation and Purification Technology*, *79*(3), 365–374. https://doi.org/10.1016/j.seppur.2011.03.025

Huang, Y. C., Fowkes, F. M., Lloyd, T. B., & Sanders, N. D. (1991). Adsorption of Calcium Ions from Calcium Chloride Solutions onto Calcium Carbonate Particles*. In *Langmuir* (Vol. 7). https://pubs.acs.org/sharingguidelines

Hube, S., Eskafi, M., Hrafnkelsdóttir, K. F., Bjarnadóttir, B., Bjarnadóttir, M. Á., Axelsdóttir, S., & Wu, B. (2020). Direct membrane filtration for wastewater treatment and resource recovery: A review. *Science of The Total Environment*, *710*, 136375. https://doi.org/10.1016/J.SCITOTENV.2019.136375

Jarusutthirak, C., & Amy, G. (2006). Role of Soluble Microbial Products (SMP) in Membrane Fouling and Flux Decline. *Environmental Science & Technology*, *40*(3), 969–974. https://doi.org/10.1021/es050987a

Jarusutthirak, C., & Amy, G. (2007). Understanding soluble microbial products (SMP) as a component of effluent organic matter (EfOM). *Water Research*, *41*(12), 2787–2793. https://doi.org/10.1016/j.watres.2007.03.005

Karar, A., Naamoune, F., & Kahoul, A. (2016). Chemical and electrochemical study of the inhibition of calcium carbonate precipitation using citric acid and sodium citrate. *Desalination and Water Treatment*, *57*(35), 16300–16309. https://doi.org/10.1080/19443994.2015.1077743

Katsoufidou, K., Yiantsios, S. G., & Karabelas, A. J. (2007). Experimental study of ultrafiltration membrane fouling by sodium alginate and flux recovery by backwashing. *Journal of Membrane Science*, *300*(1–2), 137–146. https://doi.org/10.1016/J.MEMSCI.2007.05.017

Ke, X., Hongqiang, R., Lili, D., Jinju, G., & Tingting, Z. (2013). A review of membrane fouling in municipal secondary effluent reclamation. *Environ Sci Pollut Res*, *20*, 771–777. https://doi.org/10.1007/s11356-012-1147-y

Kim, J., & van der Bruggen, B. (2010). The use of nanoparticles in polymeric and ceramic membrane structures: Review of manufacturing procedures and performance improvement for water treatment. *Environmental Pollution*, *158*(7), 2335–2349. https://doi.org/10.1016/J.ENVPOL.2010.03.024

Kirschner, A. Y., Cheng, Y. H., Paul, D. R., Field, R. W., & Freeman, B. D. (2019). Fouling mechanisms in constant flux crossflow ultrafiltration. *Journal of Membrane Science*, *574*, 65–75. https://doi.org/10.1016/j.memsci.2018.12.001

Kramer, F. C., Shang, R., Heijman, S. G. J., Scherrenberg, S. M., van Lier, J. B., & Rietveld, L. C. (2015). Direct water reclamation from sewage using ceramic tight ultra- and nanofiltration. *Separation and Purification Technology*, *147*, 329–336. https://doi.org/10.1016/j.seppur.2015.04.008

Kramer, F. C., Shang, R., Rietveld, L. C., & Heijman, S. J. G. (2020). Fouling control in ceramic nanofiltration membranes during municipal sewage treatment. *Separation and Purification Technology*, *237*, 116373. https://doi.org/10.1016/J.SEPPUR.2019.116373

Lee, M., Wu, Z., & Li, K. (2015). Advances in ceramic membranes for water treatment. In *Advances in Membrane Technologies for Water Treatment: Materials, Processes and Applications* (pp. 43–82). Elsevier Inc. https://doi.org/10.1016/B978-1-78242-121-4.00002-2

Li, C., Sun, W., Lu, Z., Ao, X., & Li, S. (2020). Ceramic nanocomposite membranes and membrane fouling: A review. In *Water Research* (Vol. 175). Elsevier Ltd. https://doi.org/10.1016/j.watres.2020.115674

Li, Q., & Elimelech, M. (2004). Organic Fouling and Chemical Cleaning of Nanofiltration Membranes: Measurements and Mechanisms. *Environmental Science & Technology*, *38*(17), 4683–4693. https://doi.org/10.1021/es0354162

Li, X., Gao, B., Yue, Q., Ma, D., Rong, H., Zhao, P., & Teng, P. (2015). Effect of six kinds of scale inhibitors on calcium carbonate precipitation in high salinity wastewater at high temperatures. *Journal of Environmental Sciences (China)*, *29*, 124–130.

https://doi.org/10.1016/j.jes.2014.09.027

Lin, B., Heijman, S. G. J., Shang, R., & Rietveld, L. C. (2021). Integration of oxalic acid chelation and Fenton process for synergistic relaxation-oxidation of persistent gel-like fouling of ceramic nanofiltration membranes. *Journal of Membrane Science*, *636*. https://doi.org/10.1016/j.memsci.2021.119553

Listiarini, K., Sun, D. D., & Leckie, J. O. (2009). Organic fouling of nanofiltration membranes: Evaluating the effects of humic acid, calcium, alum coagulant and their combinations on the specific cake resistance. *Journal of Membrane Science*, *332*(1–2), 56–62. https://doi.org/10.1016/j.memsci.2009.01.037

Mitsionis, A. I., Vaimakis, T. C., & Trapalis, C. C. (2010). The effect of citric acid on the sintering of calcium phosphate bioceramics. *Ceramics International*, *36*(2), 623–634. https://doi.org/10.1016/j.ceramint.2009.09.034

Mohammad, A. W., Teow, Y. H., Ang, W. L., Chung, Y. T., Oatley-Radcliffe, D. L., & Hilal, N. (2015). Nanofiltration membranes review: Recent advances and future prospects. In *Desalination* (Vol. 356, pp. 226–254). Elsevier. https://doi.org/10.1016/j.desal.2014.10.043

Moulin, P., & Roques, H. (2003). Zeta potential measurement of calcium carbonate. *Journal of Colloid and Interface Science*, *261*(1), 115–126. https://doi.org/10.1016/S0021-9797(03)00057-2

Mustafa, G., Wyns, K., Vandezande, P., Buekenhoudt, A., & Meynen, V. (2014). Novel grafting method efficiently decreases irreversible fouling of ceramic nanofiltration membranes. *Journal of Membrane Science*, *470*, 369–377. https://doi.org/10.1016/j.memsci.2014.07.050

Porcelli, N., & Judd, S. (2010). Chemical cleaning of potable water membranes: A review. *Separation and Purification Technology*, *71*(2), 137–143. https://doi.org/10.1016/J.SEPPUR.2009.12.007

Strathmann, H. (1981). Membrane separation processes. *Journal of Membrane Science*, *9*(1–2), 121–189.

Sun, W., Liu, J., Chu, H., & Dong, B. (2013). Pretreatment and membrane hydrophilic modification to reduce membrane fouling. *Membranes*, *3*(3), 226–241. https://doi.org/10.3390/MEMBRANES3030226

Wang, J., Cahyadi, A., Wu, B., Pee, W., Fane, A. G., & Chew, J. W. (2020). The roles of particles in enhancing membrane filtration: A review. In *Journal of Membrane Science* (Vol. 595). Elsevier B.V. https://doi.org/10.1016/j.memsci.2019.117570

Wang, J., Tang, X., Xu, Y., Cheng, X., Li, G., & Liang, H. (2020). Hybrid UF/NF process treating secondary effluent of wastewater treatment plants for potable water reuse: Adsorption vs. coagulation for removal improvements and membrane fouling alleviation. *Environmental Research*, *188*. https://doi.org/10.1016/j.envres.2020.109833

Wintgens, T., Melin, T., Schäfer, A., Khan, S., Muston, M., Bixio, D., & Thoeye, C. (2005). The role of membrane processes in municipal wastewater reclamation and reuse. *Desalination*, *178*(1–3), 1–11. https://doi.org/10.1016/J.DESAL.2004.12.014

Wu, J., Zhang, Y., Wang, J., Zheng, X., & Chen, Y. (2021). Municipal wastewater reclamation and reuse using membrane-based technologies: A review. *Desalination and Water Treatment*, *224*, 65–82. https://doi.org/10.5004/dwt.2021.27175

Xie, Z. P., Wang, X., Jia, Y., & Huang, Y. (2003). Ceramic forming based on gelation principle and process of sodium alginate. *Materials Letters*, *57*(9–10), 1635–1641. https://doi.org/10.1016/S0167-577X(02)01044-3

You, S. H., Tseng, D. H., & Hsu, W. C. (2007). Effect and mechanism of ultrafiltration membrane fouling removal by ozonation. *Desalination*, *202*(1–3), 224–230. https://doi.org/10.1016/j.desal.2005.12.058

Zazouli, M. A., Nasseri, S., & Ulbricht, M. (2010). Fouling effects of humic and alginic acids in nanofiltration and influence of solution composition. *Desalination*, *250*(2), 688–692. https://doi.org/10.1016/j.desal.2009.05.021

Zhang, W., Luo, J., Ding, L., & Jaffrin, M. Y. (2015). A Review on Flux Decline Control Strategies in Pressure-Driven Membrane Processes. *Industrial & Engineering Chemistry Research*, *54*(11), 2843–2861. https://doi.org/10.1021/ie504848m

Zhao, Y., Wang, X., Yang, H., & Xie, Y. F. (2018). Effects of organic fouling and cleaning on the retention of pharmaceutically active compounds by ceramic nanofiltration membranes. *Journal of Membrane Science*, *563*, 734–742. https://doi.org/10.1016/j.memsci.2018.06.047

Appendix

A. Duplicate of three filtration/cleaning cycles with $CaCO_3$ pre-coated membrane.

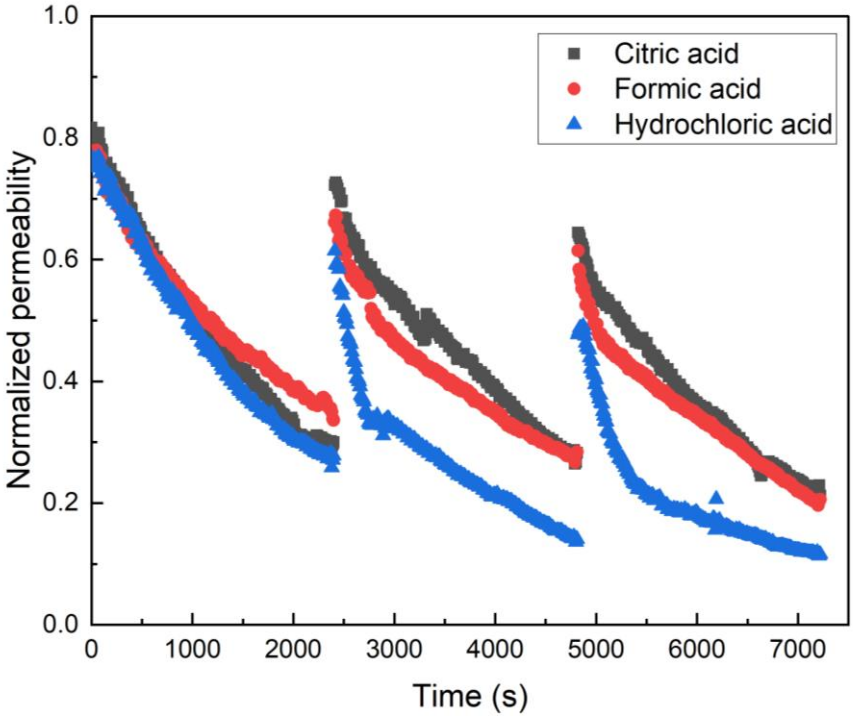

B. Duplicate of three filtration/cleaning cycles with $CaHPO_4$ & $CaCO_3$ pre-coated membrane

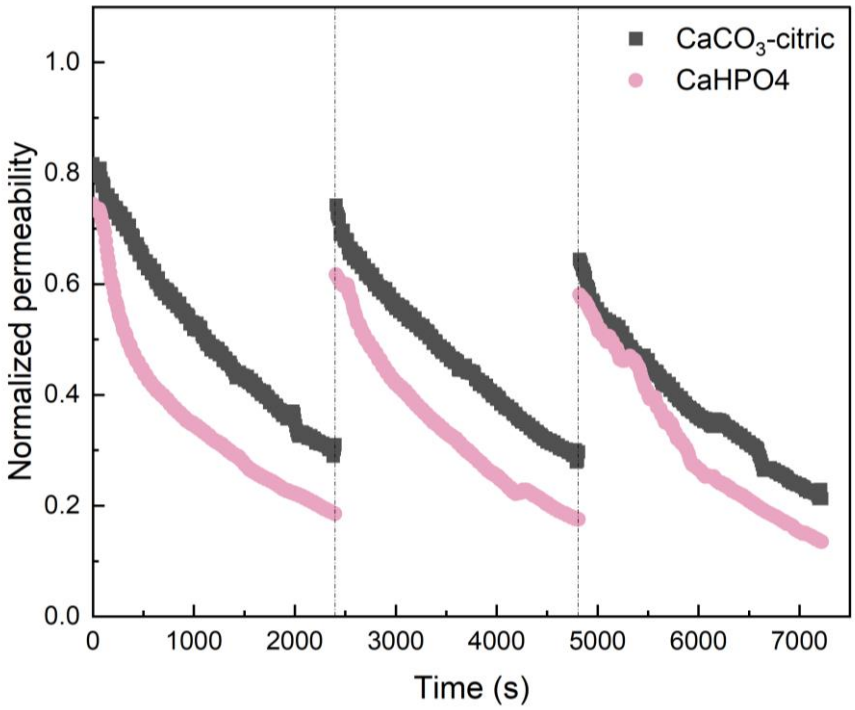

C. PSD of $Ca_3(PO_4)_2$.

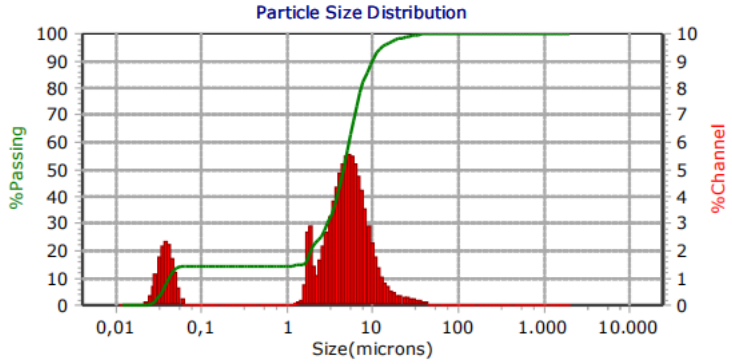

The mean size of Ca3(PO4)2 was 5.23 μm, which was too large in this experiment. As can be seen from Sec 4.4, and also from the experiments done by Yuke Li in green lab, the larger size of pre-coat particles could affect the fouling curve and efficiency of the acid cleaning.